Electronic Supplementary Information for

A novel aggregation–induced enhanced emission aromatic molecule: 2-aminophenylboronic acid dimer

Xiaopei Li,[a,b] Dongdong Wang,[a] Yongjie Zhang,[a] Wenqi Lu,[a] Songqiu Yang,[a] Guangjin Hou,[a] Zhenchao Zhao,[a] Haijuan Qin,[c] Yahui Zhang,[a] Minmin Li [a] and Guangyan Qing*[a]

[a.] *CAS Key Laboratory of Separation Science for Analytical Chemistry, Dalian Institute of Chemical Physics, Chinese Academy of Sciences, Dalian 116023, P. R. China.*

[b.] *Instrumental Analysis Center, Dalian Polytechnic University, Dalian 116034, P. R. China.*

[c.] *Research Centre of Modern Analytical Technology, Tianjin University of Science and Technology, Tianjin 300457, P. R. China.*

*Corresponding authors: qinggy@dicp.ac.cn

Outline

Materials and Measurements

Materials: 2-aminophenylboronic acid (2-APBA, 96%) was purchased from Aladdin reagent (Shanghai, P. R. China, product No. A137630) and Alfa Aesar (Product No. L18069), respectively. 4-aminophenylboronic acid hydrochloride (4-APBA·HCl, 97%, product No. A120027) and 10−hydroxybenzo[*h*]quinoline (HBQ, 98%) were purchased from Aladdin. 3-aminophenylboronic acid (3-APBA, 98%, product No.435365) was obtained from J&K Scientific. Other reagents and solvents were obtained from commercial suppliers. 4-APBA was prepared by a reaction between 4-APBA·HCl and NaOH in water. The generated NaCl was removed by a Shimadzu LC−20AT high performance liquid chromatography (HPLC) with a semi−preparative C18 reversed phase column (10 mm × 250 mm, ACCHROM Corp. P. R. China), then the solid 4-APBA sample was obtained by lyophilization. 2-APBA used for cultivating the single crystal was purified by HPLC with the above C18 column. Amorphous 2-APBA dimer sample was prepared by melting the solid 2-APBA dimer sample under a nitrogen atmosphere and then rapidly quenching the molten 2-APBA dimer with liquid nitrogen. Unless otherwise noted, other chemicals were used as received.

Luminescence measurements:

Fluorescence spectra of liquid samples were measured on a PerkinElmer LS55 fluorescence spectrometer with a 1 cm path−length quartz cell. The fluorescence spectra of solid samples were measured on a PerkinElmer FL6500 fluorescence spectrometer. Fluorescence absolute quantum yields (Φ_F) of the liquid and solid samples were determined by an Edinburgh FLS980 spectrometer with an integrating sphere. Time resolved fluorescence decays of the liquid and solid samples were also conducted on the Edinburgh FLS980 spectrometer using a time−correlated single photon counting (TCSPC) method, and data analysis, where single−exponential function (Eq.S1) or double−exponential function (Eq.S2) was adopted,[1] was performed with a software package provided by the Edinburgh instrument.

$$y = \alpha e^{-t/\tau} \tag{S1}$$

$$y = \alpha_1 e^{-t/\tau_1} + \alpha_2 e^{-t/\tau_2} \tag{S2}$$

Where τ is a fluorescence lifetime, α_1 and α_2 represent the fractional amounts of molecules with τ_1 and τ_2, respectively.

Absolute Φ_F and τ can be expressed as follows: [2]

$$\Phi_F = \frac{k_F}{k_F + k_{nr}} = \frac{k_F / k_{nr}}{k_F / k_{nr} + 1} \quad \text{(S3)}$$

$$\tau = \frac{1}{k_F + k_{nr}} \quad \text{(S4)}$$

Where k_F is the radiative decay rate constant. k_{nr} is the total nonradiative decay rate constant.

When there are two τ values, Eq.S4 turns into the following expression.

$$\langle \tau \rangle = \frac{1}{k_F + k_{nr}} \quad \text{(S5)}$$

Where

$$\langle \tau \rangle = \frac{\alpha_1 \tau_1^{\,2} + \alpha_2 \tau_2^{\,2}}{\alpha_1 \tau_1 + \alpha_2 \tau_2} \quad \text{(S6)}$$

Where <τ> refers to the average fluorescence lifetime. Based on Eqs. S3-S6, values of k_F and k_{nr} can be obtained.

SEM measurements: SEM measurements were carried out on a JEOL JSM−7800 F instrument and the elemental compositions were analyzed by an X−ray energy dispersive spectroscopy (EDS) (X−Max50, Oxford), which is connected with the JSM−7800 F instrument. For the liquid samples, SEM samples were prepared by dripping several drops of solution onto clean silicon wafers and evaporating the solvent at room temperature and in open air. For solid samples, SEM samples were prepared by directly sticking the powder on the carbon tapes.

XRD measurements: Powder XRD patterns were collected by a Shimadzu XRD−7000S Powder X−ray diffractometer with 1.5418 Å Cu K_α radiation (scan speed: 5°/min; scan range: 5–80°). The single−crystal XRD data for 2-APBA were collected on a Bruker D8 Venture CMOS−based diffractometer (Mo–Kα radiation, λ=0.71073 Å) using the SMART and SAINT programs at 120 K. Final unit cell parameters were based on all observed reflections from integration of all frame data. The structure was

solved in the space group by direct method and refined by the full−matrix least−squares using SHELXTL−97 fitting on F^2. All non−hydrogen atoms were refined anisotropically. The hydrogen atoms were located geometrically and assigned fixed isotropic thermal parameters.[3]

NMR measurements: ^{11}B MAS NMR spectra of the solid samples were recorded on a Bruker AVANCE Ⅲ 600 MHz spectrometer, using a 4-mm double resonance HX MAS NMR probe with a spinning rate of 12 kHz and a small flip angle of π/12 pulse. The spectra were accumulated with 64 scans, a recycle delay of 20 s. The chemical shifts were referenced to a 0.1 M H_3BO_3 aqueous solution at 19.6 ppm.[4] $^1H–^{15}N$ CP−MAS NMR spectra of solid sample were acquired on a Bruker AVANCE III 400 MHz spectrometer, using a 7 mm double resonance HX MAS NMR probe with a spinning rate of 4 kHz. The spectra were accumulated with 2048 scans, a recycle delay of 60 s. The chemical shifts were referenced to glycine at 33.4 ppm.[5] ^1H, ^{13}C, $^1H–^1H$ COSY, $^1H–^1H$ NOESY, $^1H–^{13}C$ HSQC and $^1H–^{13}C$ HMBC NMR experiments were performed on a Bruker AVANCE III 400 spectrometer equipped with a 5 mm BBFO probe.

Particle size measurements: NanoSight NS300 instrument (Malvern Panalytical Corp.) with a monochromatic laser beam at 488 nm was used to confirm whether there were particles in the 2-APBA dimer, 3- and 4-APBA aqueous solution. Each experimental run with 30 s duration was performed in quintuplicate. The velocity of particle movement was used to calculate particle sizes (d_h, hydrodynamic diameter) by applying the two−dimensional Stokes−Einstein equation (Eq.S7).[6] The data were analyzed by NTA 3.3 software (NanoSight).

$$\langle x, y \rangle^2 = \frac{K_B T t_s}{3\pi\eta d_h} \quad \text{(S7)}$$

Where $\langle x, y \rangle^2$ is the mean squared displacement, K_B is Boltzmann's constant, T is the temperature in Kelvin, t_s is the sampling time, η is the viscosity, and d_h is the hydrodynamic diameter.

Theoretical calculations: Becke's three−parameter hybrid exchange function with the

Lee−Yang−Parr gradient−corrected correlation functional (B3LYP), in combination with the triple−ζ valence quality with one set of polarization functions (TZVP), was adopted for the calculation with a DFT/TDDFT method by the Gaussian 09 program.

Transmembrane ionic current measurements: Firstly, a small piece of PEI nanochannel membrane was mounted between two tailor-made Teflon modules (its center hole is 5 mm in diameter) in a stainless-steel holding apparatus. Both chambers of two Teflon modules were filled with 0.1 M KCl solution containing 2-APBA dimer aggregates (5.0×10^{-3} mol•L^{-1}) as the electrolyte. Transmembrane ionic current measurements were carried out in a Keithley 6487 picoammeter, and Ag/AgCl electrodes were used to apply a transmembrane potential across the PET nanochannel membrane. The anode and cathode, respectively, faced the large and small opening side, and the sweep voltage varied from –2 V to +2 V with a step voltage of 0.2 V and a step time of 1 s. The ionic currents obtained from the injection of 0.1 M KCl solution containing 2-APBA dimer aggregates were assigned as the initial current value (i.e., the blank current). Then, the chambers were alternately bubbled with CO_2 (20 min) and N_2 (40 min), and the corresponding ionic currents were recorded after each gas bubbling. Each measurement was repeated five times to obtain the average current values at different voltages.

Figures:

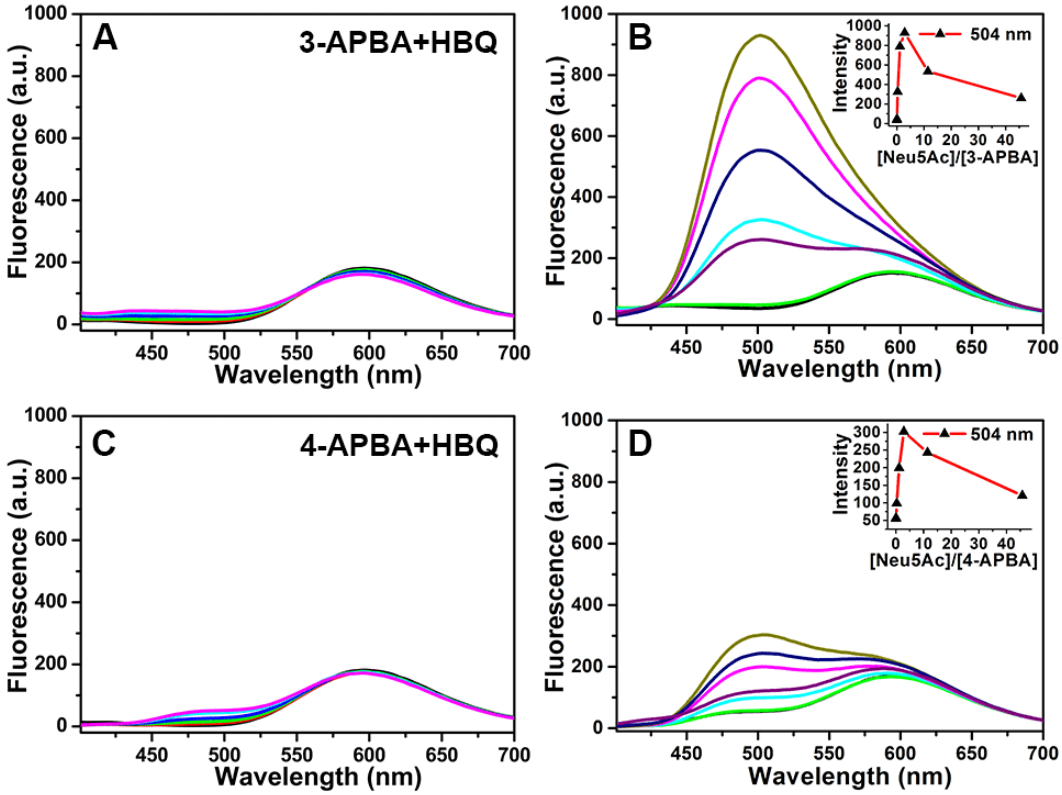

Fig. S1 (A, C) Fluorescence spectra of HBQ (5.0×10^{-5} mol L^{-1}) on addition of various equivalents of 3- or 4-APBA to the water–DMSO (4:1, v/v) solution of HBQ. (B, D) Fluorescence spectra and intensity changes (at 504 nm, inset) of HBQ–3-APBA mixture (B) or HBQ–4-APBA mixture (D) on addition of various equivalents of Neu5Ac to the water–DMSO (4:1, v/v) solution of HBQ–3-APBA or HBQ–4-APBA. λ_{ex}=367 nm. The concentration of HBQ, 3-APBA and 4-APBA were 5.0×10^{-5}, 3.5×10^{-4} and 3.5×10^{-4} mol·L^{-1}, respectively.

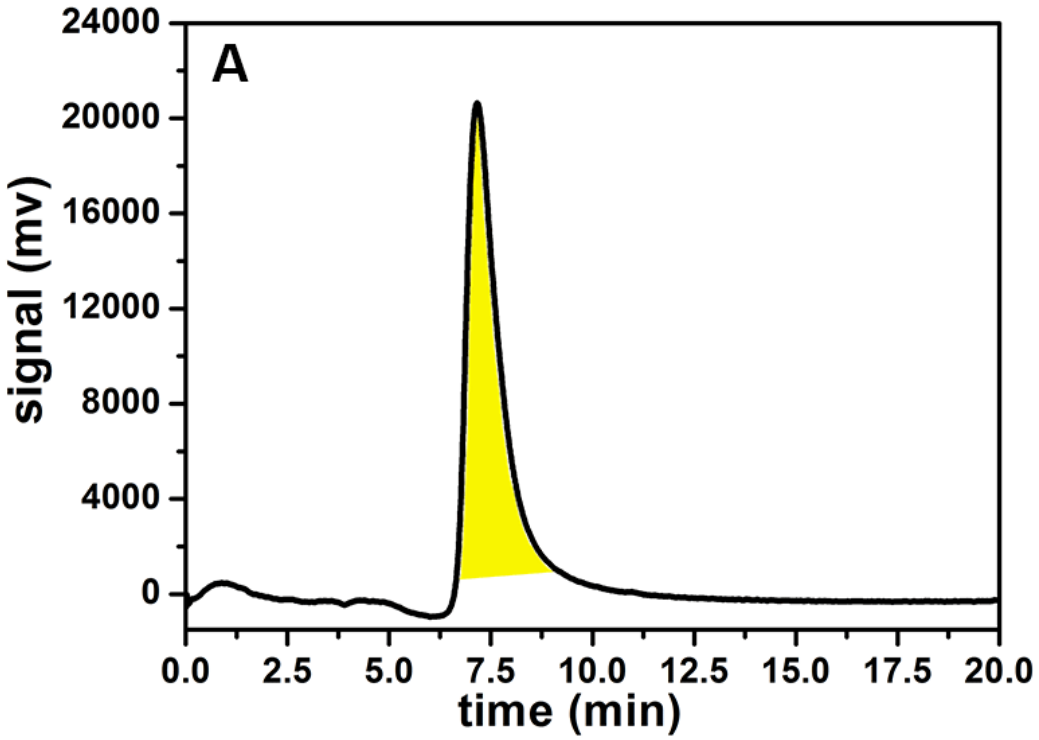

Fig. S2 HPLC spectrum of 2-APBA. To cultivate high−quality crystal, 2-APBA chemical (Aladdin reagent, Shanghai, Product No. A137630) was purified. 2-APBA was dissolved in acetonitrile, then the solution was injected into a semi−preparative C18 reversed−phase column. The effluent between 6.7 and 9.0 minute (filled with a yellow color) was collected together. A gradient elution method was applied: Firstly, a linear gradient of 30%−60% acetonitrile from 0–6 minute at a flow rate of 3 mL·min^{-1} was adopted, then a linear gradient of 60%−90% acetonitrile from 6−20 minute at a flow rate of 3 mL·min^{-1} was adopted.

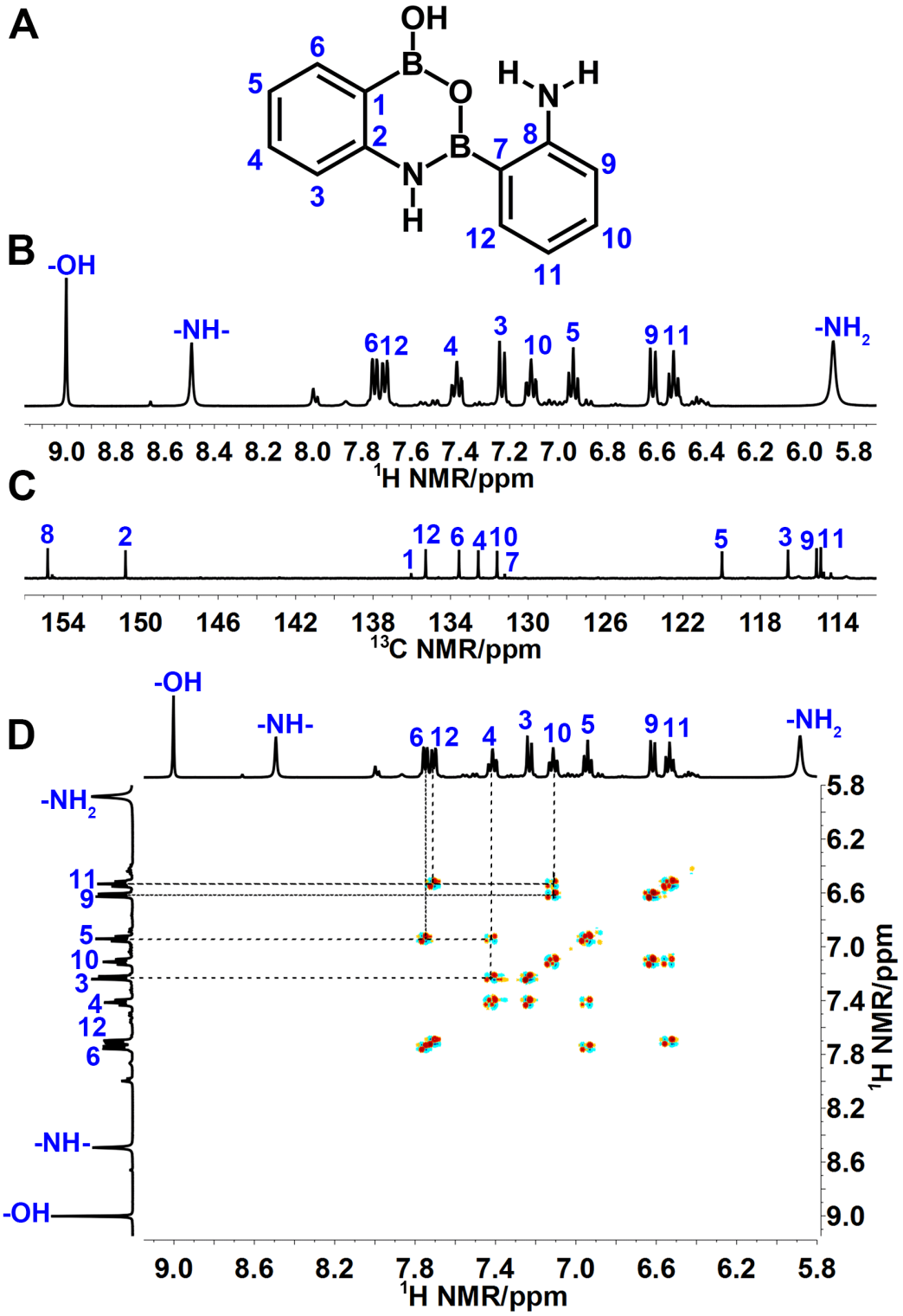
A
OH
B
O
H
N
H
B
N
H
1
2
3
4
5
6
7
8
9
10
11
12
B
-OH
-NH-
6 12
4
3
10
5
9 11
-NH2
9.0 8.8 8.6 8.4 8.2 8.0 7.8 7.6 7.4 7.2 7.0 6.8 6.6 6.4 6.2 6.0 5.8
1H NMR/ppm
C
8
2
12 6 4 10
1
7
5
3 9 11
154 150 146 142 138 134 130 126 122 118 114
13C NMR/ppm
D
-OH
-NH-
6 12
4
3
10
5
9 11
-NH2
-NH2
11
9
5
10
3
4
12
6
-NH-
-OH
5.8
6.2
6.6
7.0
7.4
7.8
8.2
8.6
9.0
1H NMR/ppm
9.0 8.6 8.2 7.8 7.4 7.0 6.6 6.2 5.8
1H NMR/ppm

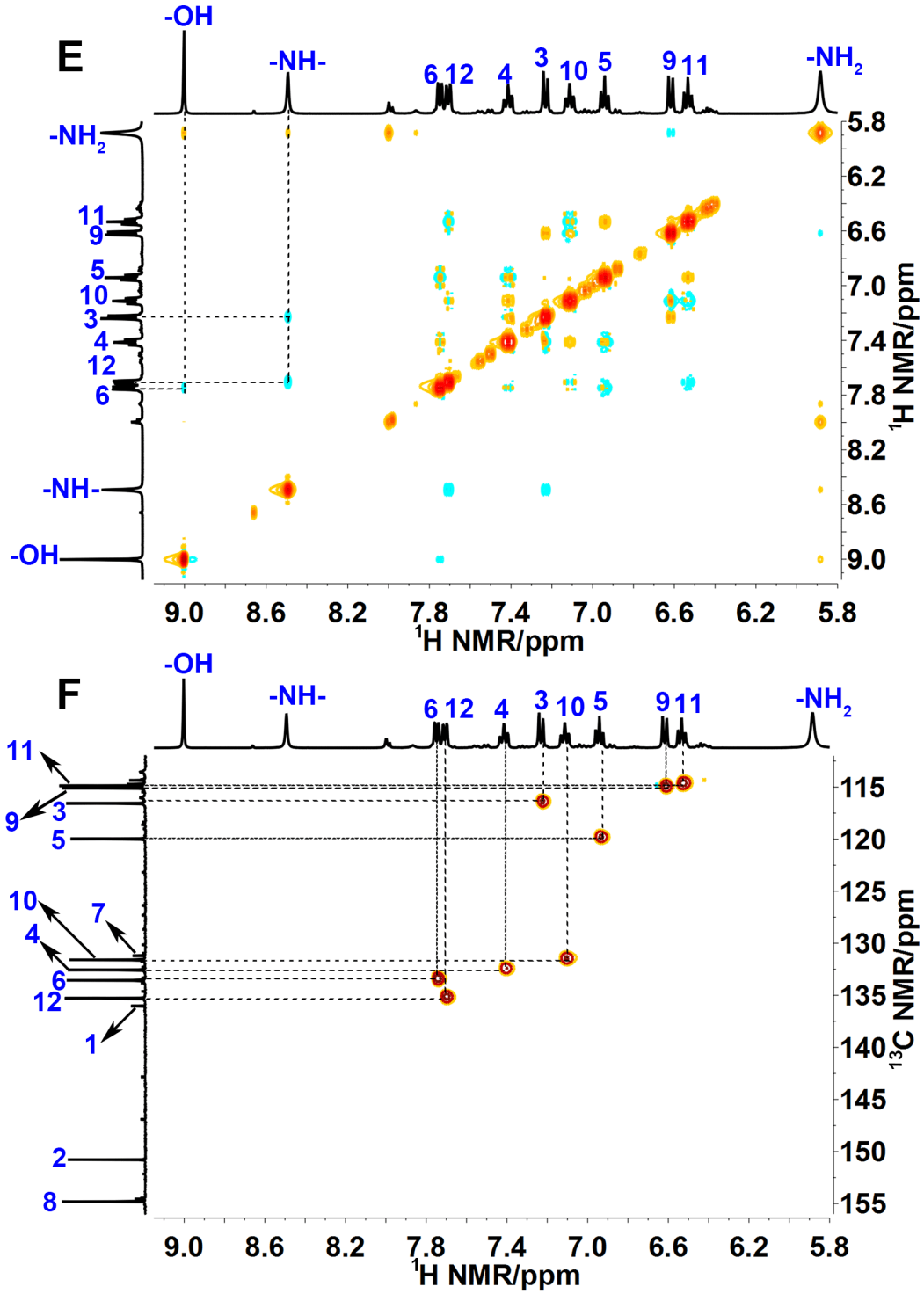
E
-OH
-NH-
6 12
4
3
10
5
9 11
-NH2
-NH2
11
9
5
10
3
4
12
6
-NH-
-OH
5.8
6.2
6.6
7.0
7.4
7.8
8.2
8.6
9.0
1H NMR/ppm
9.0 8.6 8.2 7.8 7.4 7.0 6.6 6.2 5.8
1H NMR/ppm
F
-OH
-NH-
6 12
4
3
10
5
9 11
-NH2
11
9
3
5
10
7
4
6
12
1
2
8
115
120
125
130
135
140
145
150
155
13C NMR/ppm
9.0 8.6 8.2 7.8 7.4 7.0 6.6 6.2 5.8
1H NMR/ppm

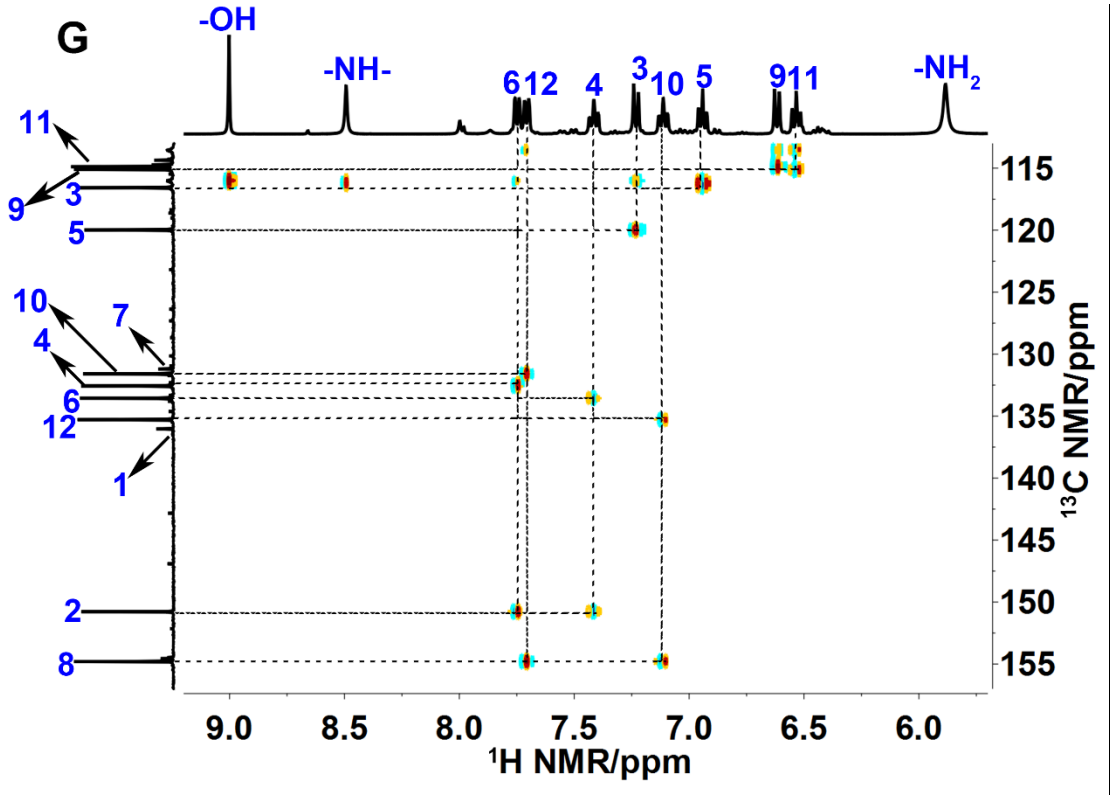

Fig. S3 Chemical structure of 2-APBA dimer (A) and ^{1}H (B), ^{13}C (C), ^{1}H–^{1}H COSY (D), ^{1}H–^{1}H NOESY (E), ^{1}H–^{13}C HSQC (F), ^{1}H–^{13}C HMBC (G) NMR spectra of 2-APBA dissolved in DMSO−d_6 at 20 °C. Concentration: 40 mg·mL^{-1}.

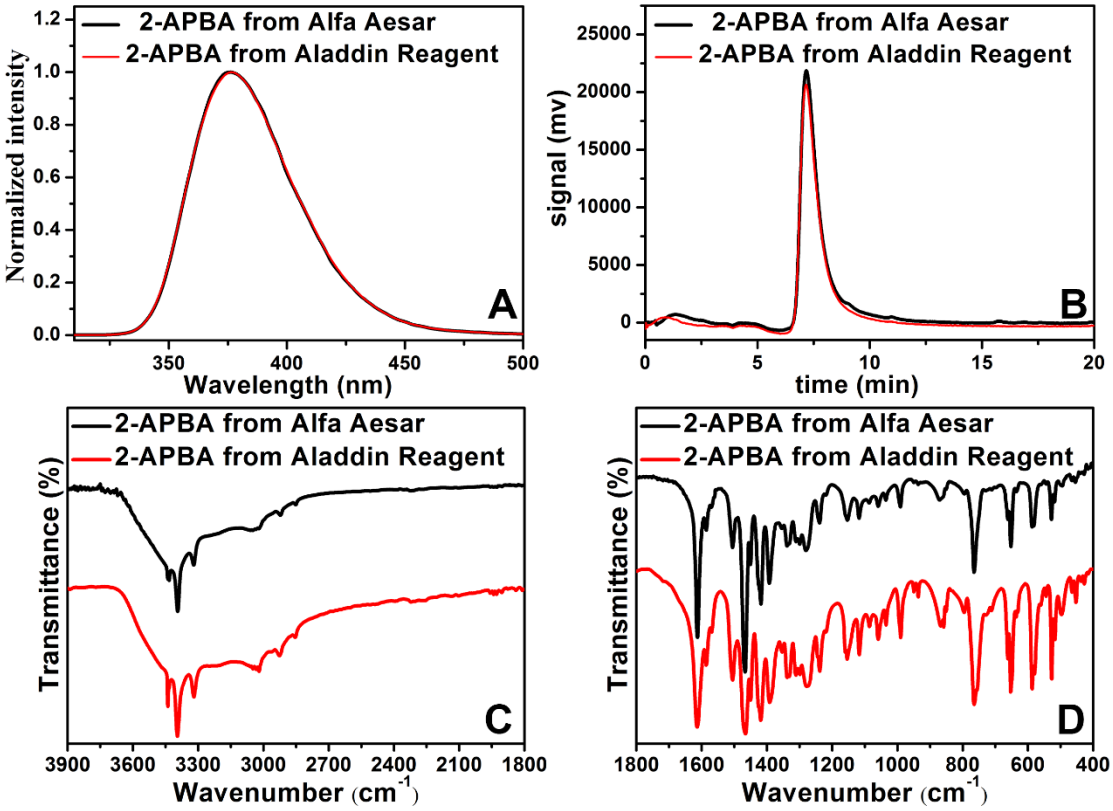
2-APBA from Alfa Aesar
2-APBA from Aladdin Reagent
Normalized intensity
Wavelength (nm)
A
signal (mv)
time (min)
B
Transmittance (%)
Wavenumber (cm-1)
C
D

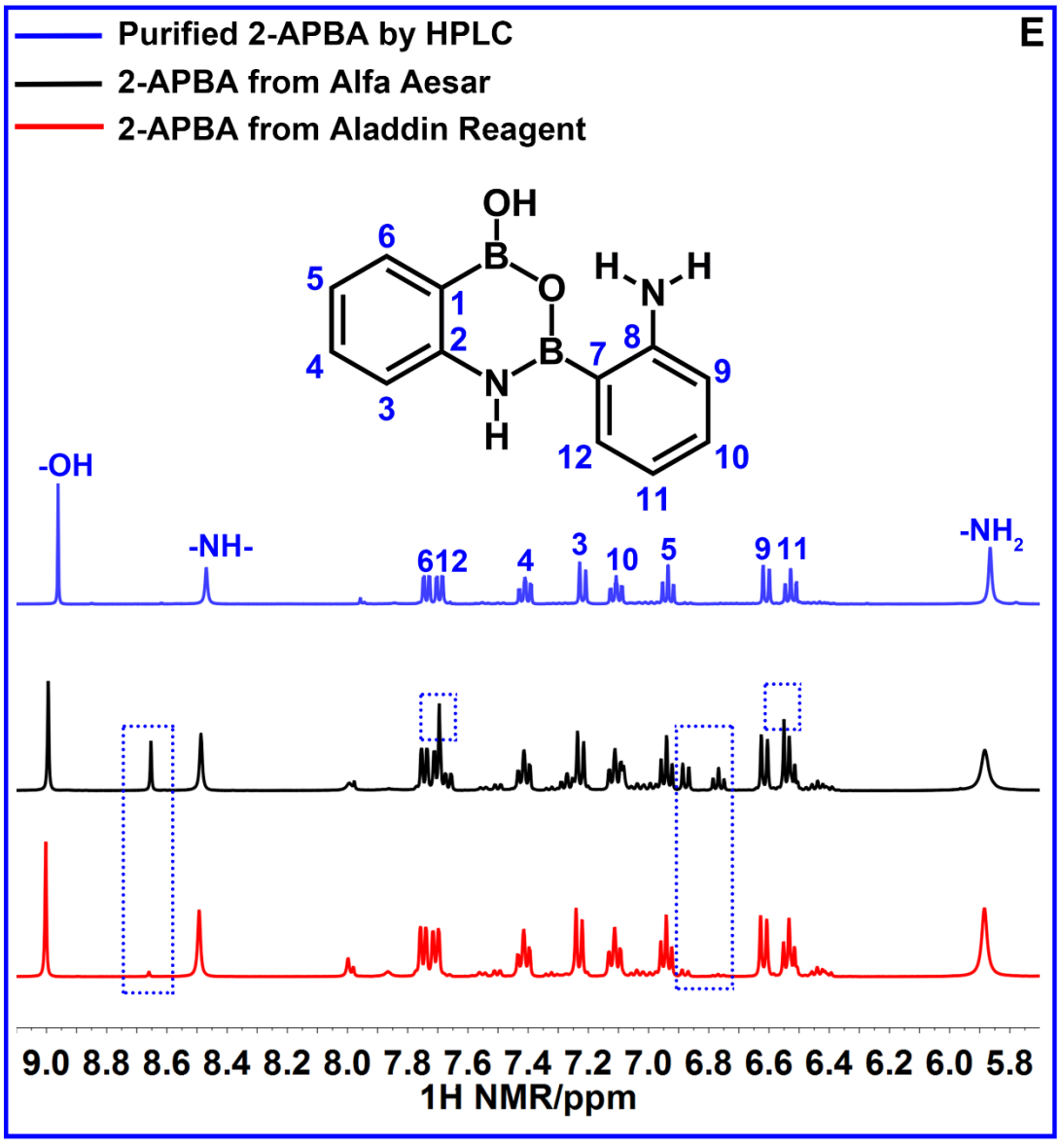
Purified 2-APBA by HPLC
2-APBA from Alfa Aesar
2-APBA from Aladdin Reagent
E
OH
B
O
H
N
H
-OH
-NH-
-NH2
1H NMR/ppm

Fig. S4 (A-D) Comparison of fluorescence spectra (A), HPLC spectra (B), FT-IR spectra in 3900-1800 range (C) and FT-IR spectra in 1800-400 range (D) of 2-APBA from Aladdin reagent and Alfa Aesar. For the fluorescent test or the HPLC separation, the samples were dissolved in water (5.0×10^{-5} mol·L^{-1}) or in acetonitrile, respectively. The 2-APBA acetonitrile solution was injected into a semi−preparative C18 reversed−phase column. A gradient elution method was applied: Firstly, a linear gradient of 30%−60% acetonitrile from 0–6 minute at a flow rate of 3 mL·min^{-1} was adopted, then a linear gradient of 60%−90% acetonitrile from 6–20 minute at a flow rate of 3 mL·min^{-1} was adopted. The fluorescence and FT-IR spectrum of 2-APBA from Alfa Aesar were the same as these of 2-APBA from Aladdin reagent. 2-APBA from Alfa Aesar possessed the same retention time as 2-APBA from Aladdin reagent. (E) ^{1}H NMR spectra of the purified 2-APBA, 2-APBA chemical from Alfa Aesar and Aladdin reagent dissolved in DMSO−d_6 at 20 ^{o}C. Concentration: 40 mg·mL^{-1}.

Discussion: The ^{1}H resonance signals of 2-APBA dimer, which were well assigned based on the ^{1}H–^{1}H COSY, ^{1}H–^{1}H NOESY, ^{1}H–^{13}C HSQC and ^{1}H–^{13}C HMBC NMR spectra of 2-APBA from Aladdin reagent (**Fig. S3**), could all be observed in the ^{1}H NMR spectrum of 2-APBA from Alfa Aesar. By comparing ^{1}H NMR spectra of the 2-APBA from Aladdin reagent and Alfa Aesar with one purified by HPLC (Fig. S4E), it can be obtained that 2-APBA from Aladdin reagent had a higher purity than that from Alfa Aesar. Thus, unless otherwise noted, 2-APBA from Aladdin reagent was used as received.

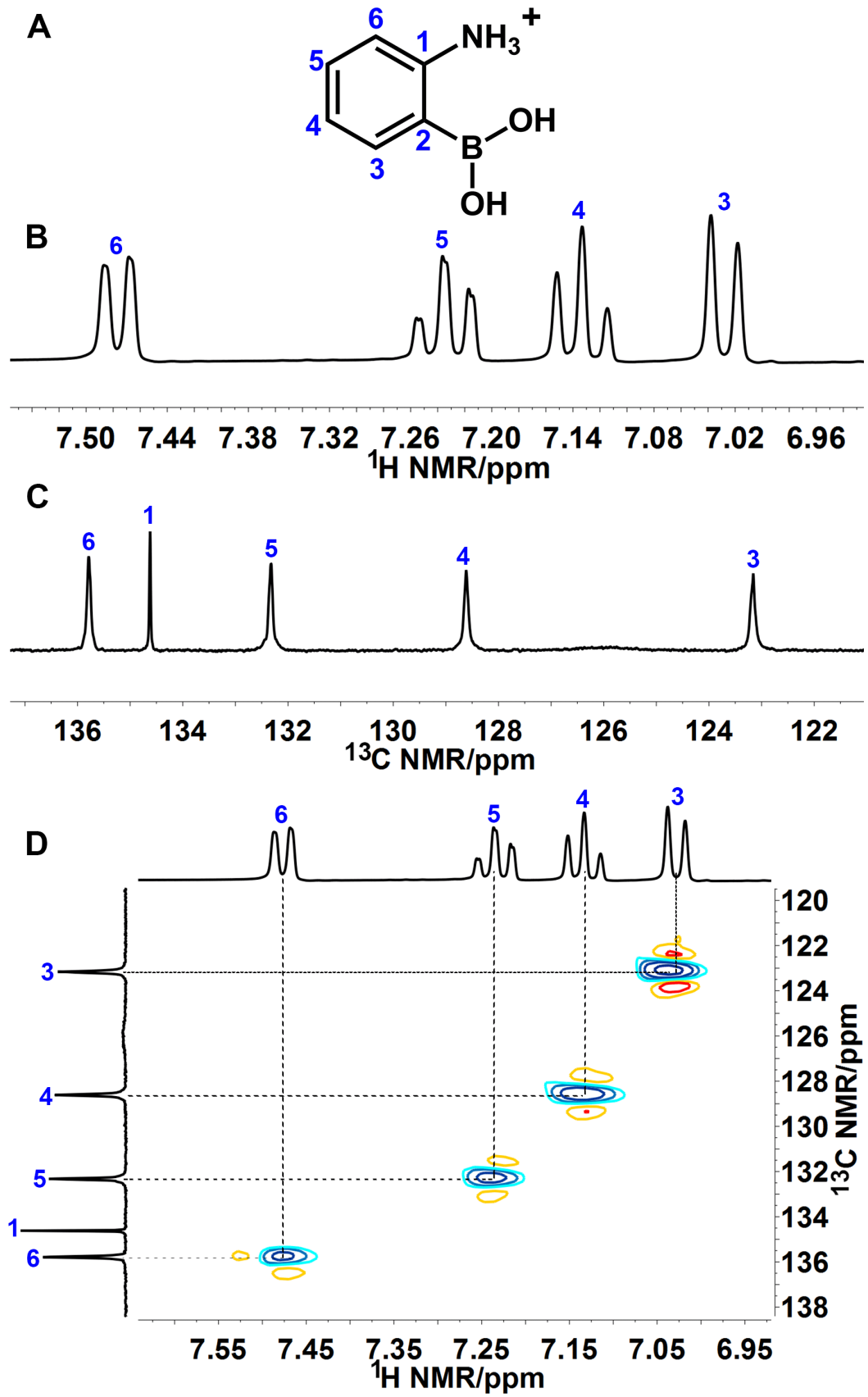
A
6
1
NH3
+
5
4
2
B
OH
3
OH
B
6
5
4
3
7.50 7.44 7.38 7.32 7.26 7.20 7.14 7.08 7.02 6.96
1H NMR/ppm
C
6
1
5
4
3
136 134 132 130 128 126 124 122
13C NMR/ppm
D
6
5
4
3
3
4
5
1
6
120
122
124
126
128
130
132
134
136
138
13C NMR/ppm
7.55 7.45 7.35 7.25 7.15 7.05 6.95
1H NMR/ppm

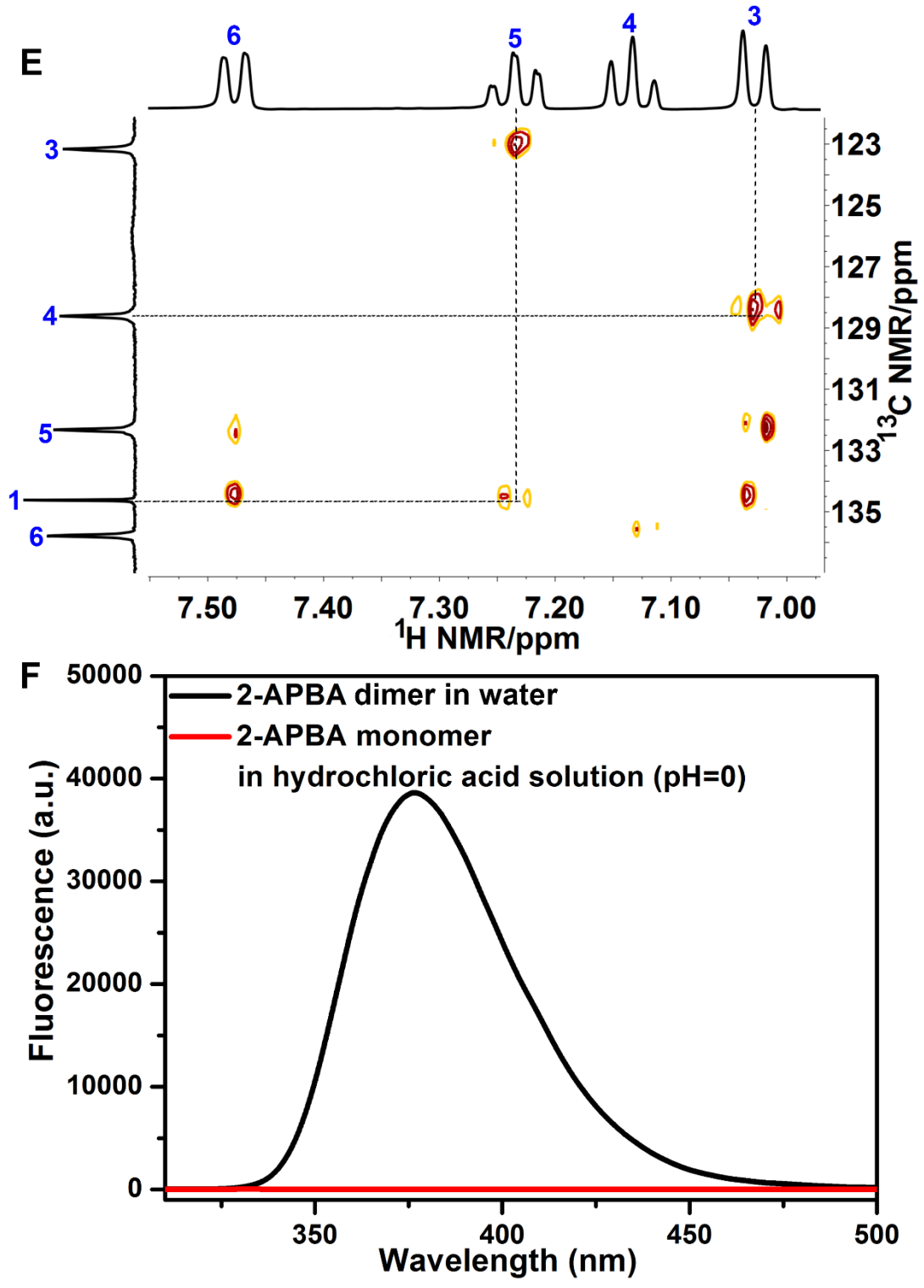

Fig. S5 (A-E) Chemical structure (A) and ^{1}H (B), ^{13}C (C), ^{1}H–^{13}C HSQC (D), ^{1}H–^{13}C HMBC (E) NMR spectra of 2-APBA dissolved in the solution of D_2O/concentrated hydrochloric acid (10:1, v/v) at 20 °C. Concentration: 40 mg·mL^{-1}. (F) Fluorescence spectra of 2-APBA dimer in water and 2-APBA monomer in hydrochloric acid solution (pH≈0), λ_{ex}=300 nm. The concentration of 2-APBA dimer and 2-APBA monomer was

5.0×10^{-5} mol·L^{-1} and 1.0×10^{-4} mol·L^{-1}, respectively. The 2-APBA monomer in hydrochloric acid solution (pH≈0) was non-emissive.

Discussion: 2-APBA was highly soluble in hydrochloric acid solution, and the NMR spectra clearly showed that 2-APBA existed in a monomeric form in hydrochloric acid solution (pH≈0).

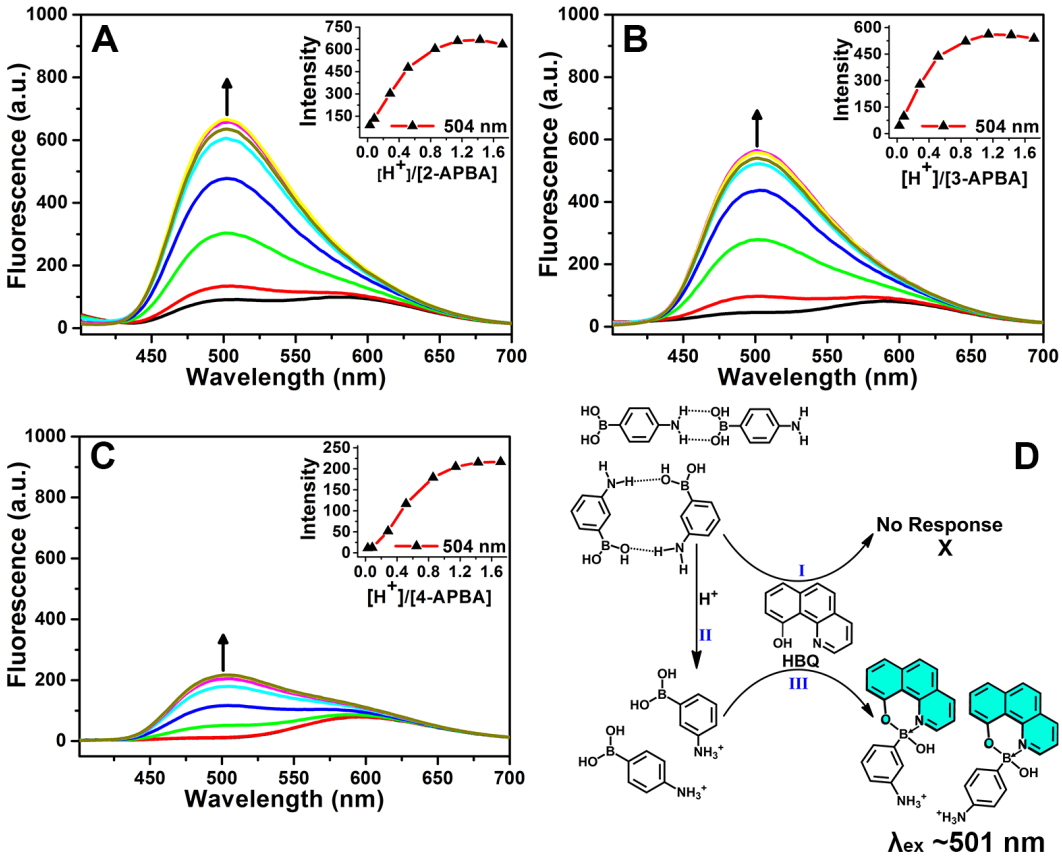

Fig. S6 (A–C) Fluorescence spectra and intensity changes (at 504 nm, inset) of HBQ–2-APBA mixture (A), HBQ–3-APBA mixture (B) or HBQ–4-APBA mixture (C) on addition of various equivalents of H^+ to the water/DMSO (4:1, v/v) solution of HBQ–2-APBA, HBQ–3-APBA or HBQ–4-APBA. λ_{ex}=367 nm. The concentration of HBQ, 2-APBA, 3-APBA and 4-APBA were 5.0×10^{-5}, 3.5×10^{-4}, 3.5×10^{-4} and 3.5×10^{-4} mol·L^{-1}, respectively. (D) Possible luminescence behavior of HBQ in response to 3-, 4-APBA and H^+.

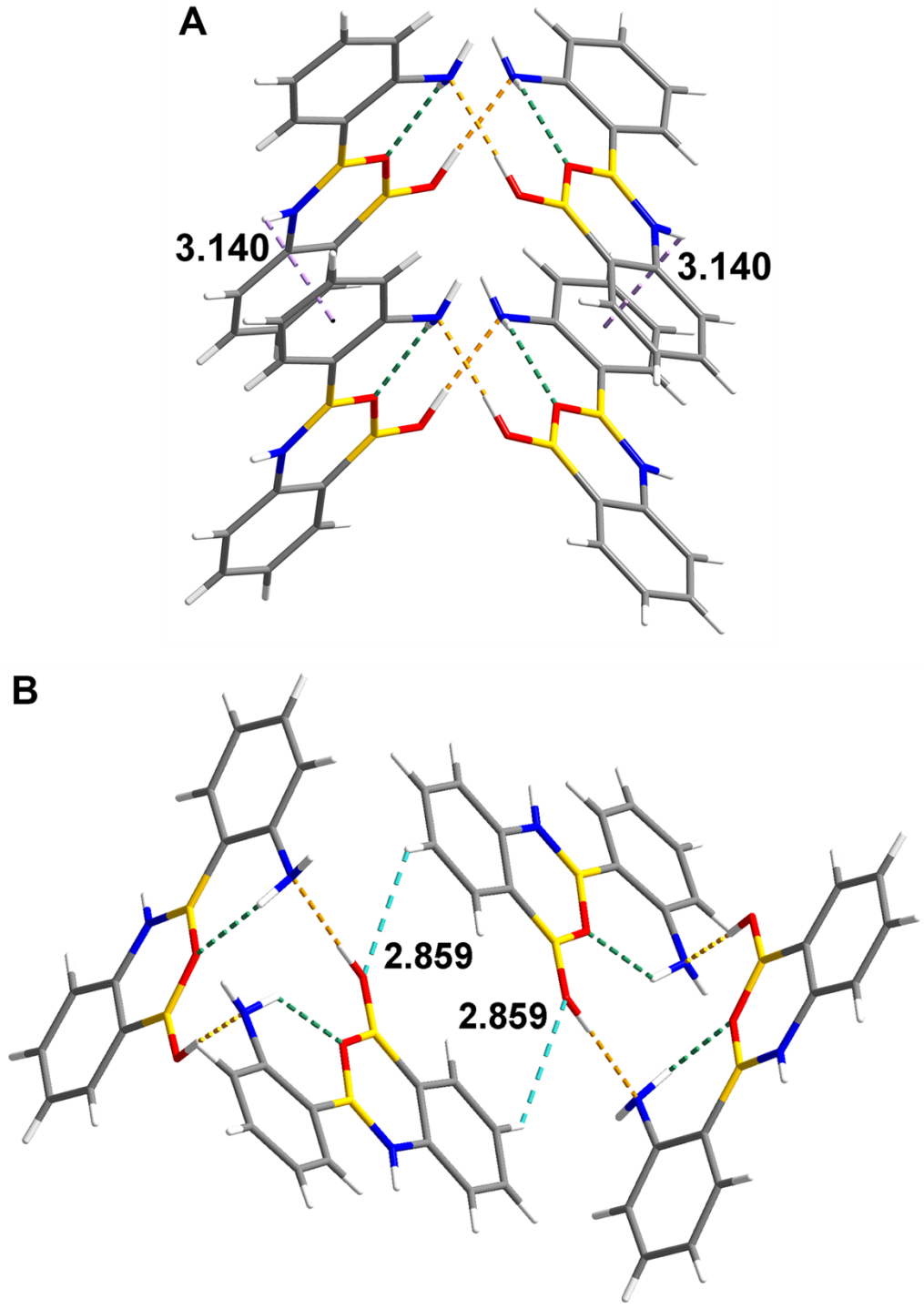

Fig. S7 (A) N−H…π interactions (dashed purple lines) with the distance of 3.140 Å in the crystal packing of 2-APBA. The angle of the N−H···ring was *ca*. 103°. (B) C−H…O hydrogen bonds (dashed turquoise line) with the distance of 2.859 Å in the crystal packing of 2-APBA.

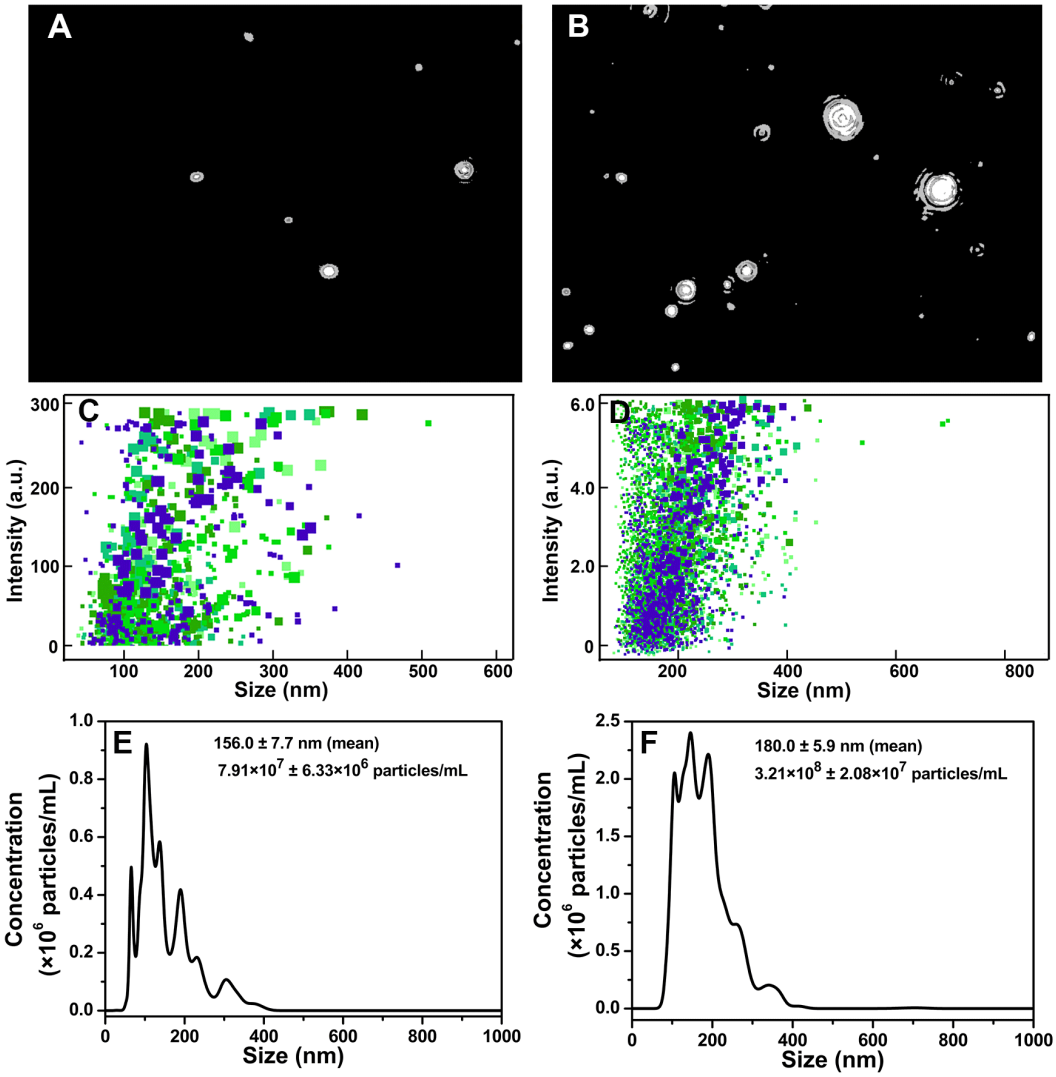

Fig. S8 A typical particle image in a 2-APBA dimer aqueous solution with a concentration of 2.9×10^{-5} mol L^{-1} (A, movie S1) or 1.2×10^{-3} mol L^{-1} (B, movie S2). Size distribution graphs of 2-APBA dimer aqueous solution with the concentration of 2.9×10^{-5} mol L^{-1} (C and E) and 1.2×10^{-3} mol L^{-1} (D and F). C and D: intensity versus size, a dot represents a particle. E and F: averaged FTLA (finite track length adjustments) concentration versus size.

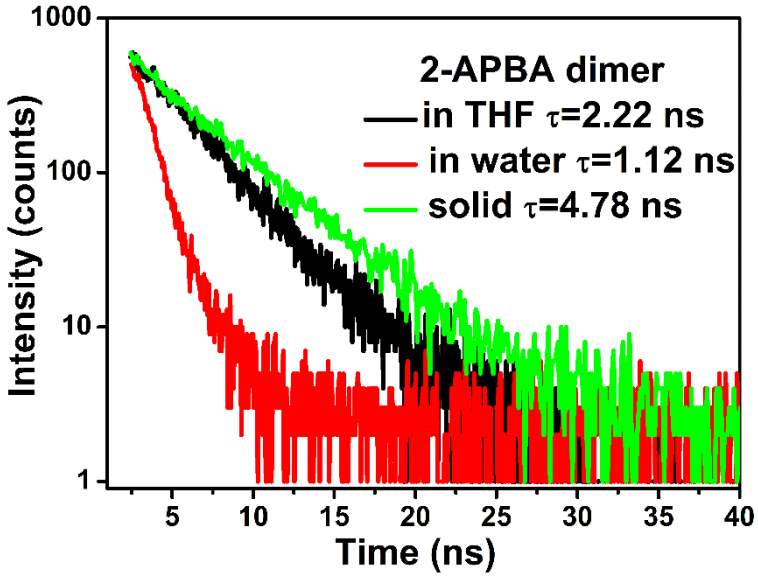

Fig. S9 Fluorescence intensity decays of 2-APBA dimer in THF, water and the solid state.

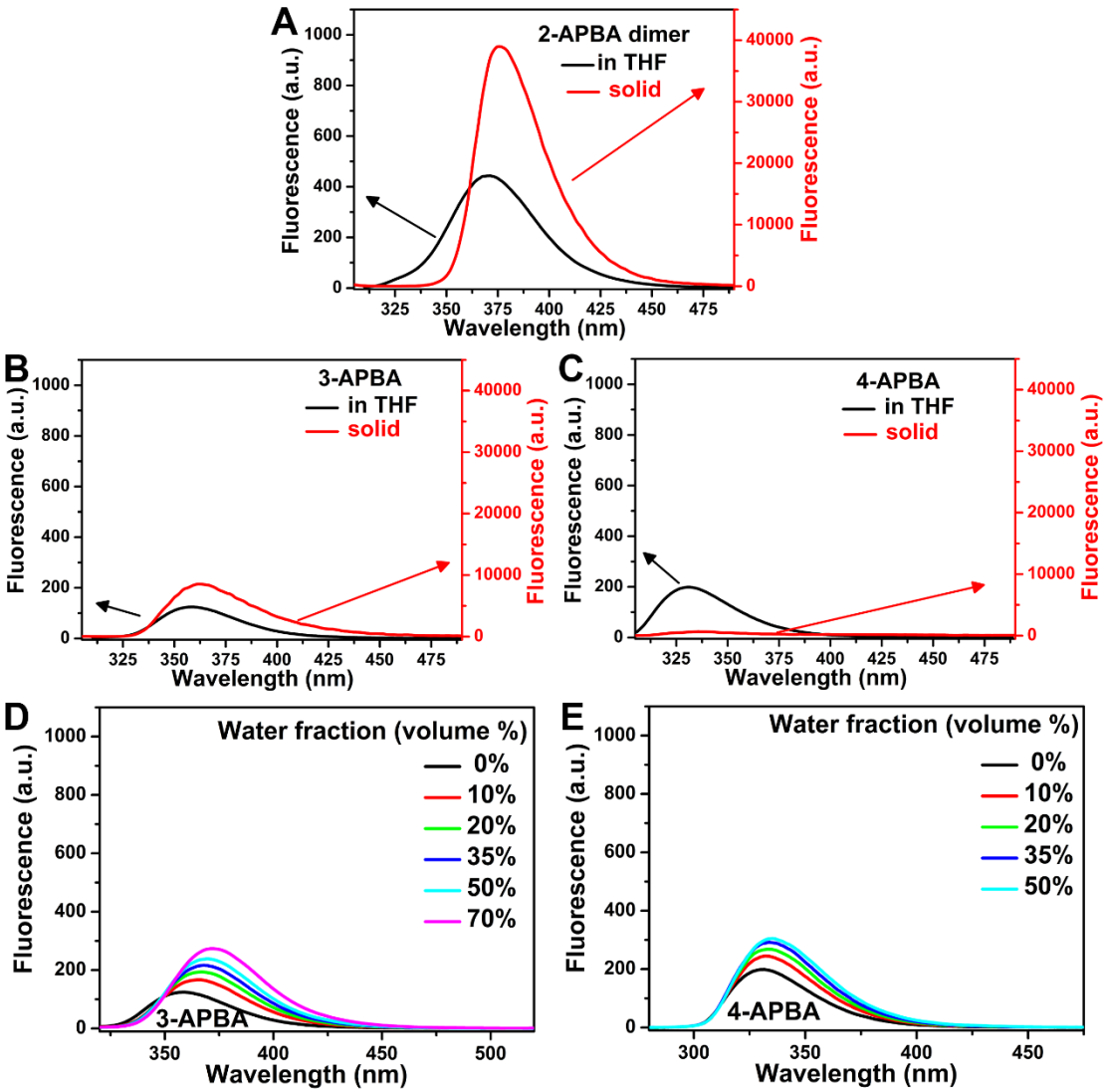

Fig. S10 (A-C) Fluorescence spectra of 2-APBA dimer (A), 3- (B) and 4-APBA (C) in THF (5.0×10^{-5} mol·L^{-1}) and the solid state. (D-E) Fluorescence spectra of 3- and 4-APBA (5.0×10^{-5} mol·L^{-1}) in THF–water mixtures with different amounts of water (volume %). 2-APBA dimer, λ_{ex}=300 nm; 3-APBA, λ_{ex}=295 nm; 4-APBA, λ_{ex}=252 nm.

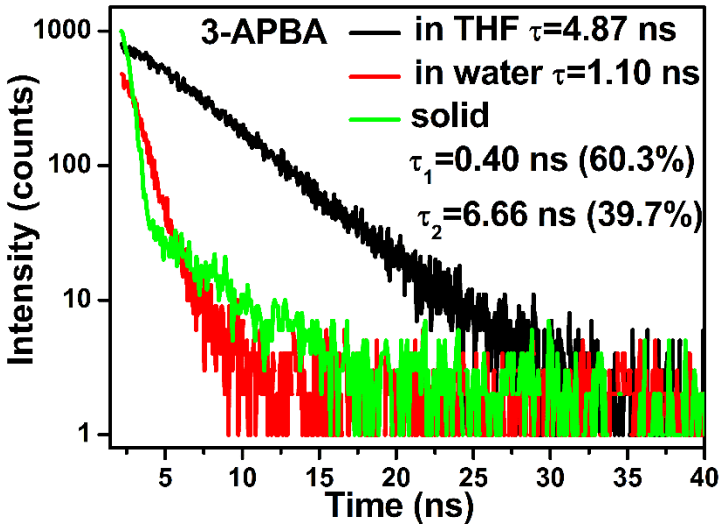

Fig. S11 Fluorescence intensity decays of 3-APBA in THF, water and the solid state.

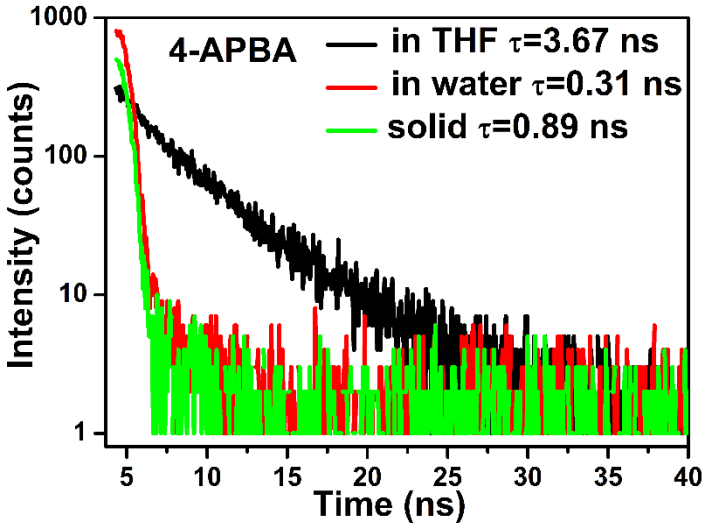

Fig. S12 Fluorescence intensity decays of 4-APBA in THF, water and the solid state.

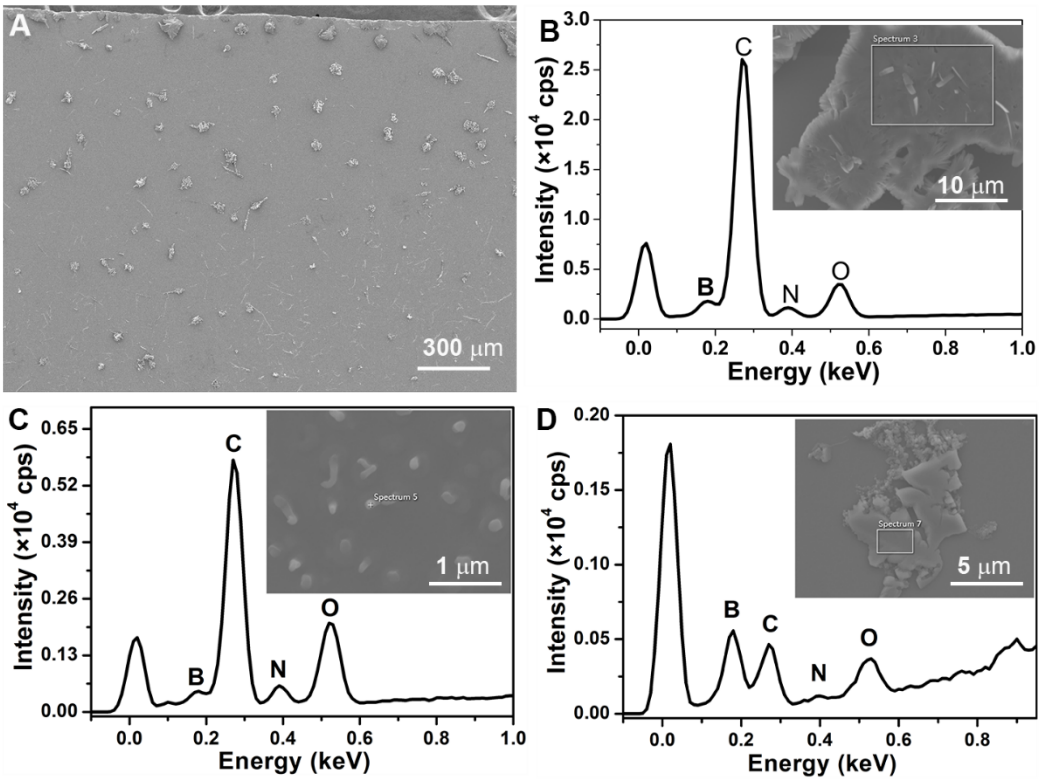

Fig. S13 (A, B) SEM image (A) and EDS spectrum (B) of 2-APBA dimer sample on silicon wafer prepared from 2-APBA dimer aqueous solution. The "Spectrum 3" in inset of **Fig. S13 B** was the place where the EDS spectrum was collected. (C) EDS spectrum of 3-APBA sample on silicon wafer prepared from 3-APBA aqueous solution. The "Spectrum 5" in inset was the place where the EDS spectrum was collected. (D) EDS spectrum of 4-APBA sample on silicon wafer prepared from 4-APBA aqueous solution. The "Spectrum 7" in inset was the place where the EDS spectrum was collected.

Discussion: Fig. 13A demonstrated that 2-APBA dimer particles in water tended to aggregate on the edge of the silicon wafer during the evaporation of the water. Clear B, C, N and O signals could be observed in the EDS spectra of 2-APBA dimer, 3- and 4-APBA on the silicon wafer, which validated that **Fig. 4** (C, H and J) in the main text were the SEM image of 2-APBA dimer, 3- and 4-APBA sample rather than the possible contamination on the silicon wafer.

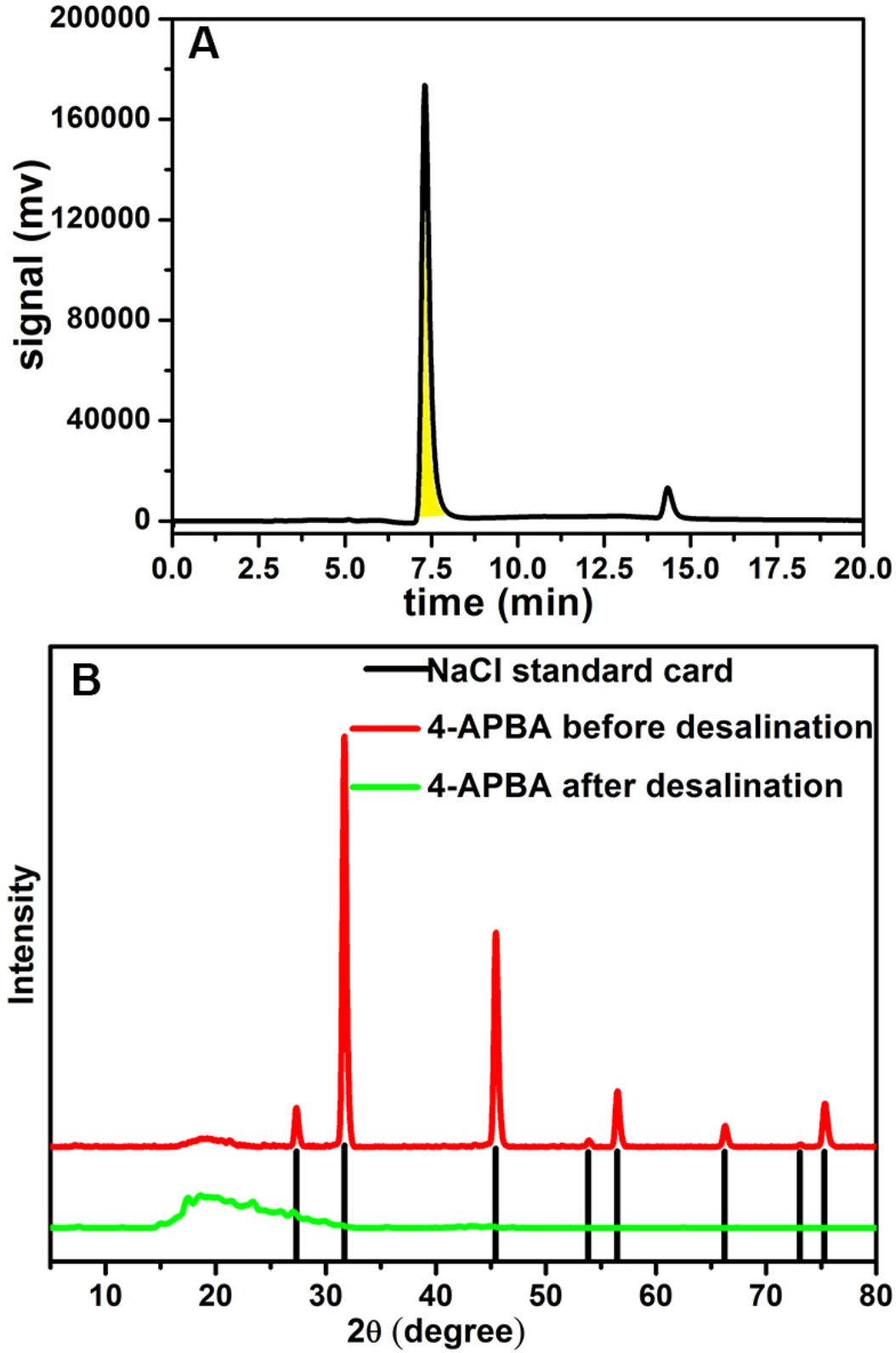

Fig. S14 (A) HPLC spectrum of 4-APBA. HPLC was used to remove NaCl from 4-APBA aqueous solution which was injected into a semi−preparative C18 reversed−phase column. The effluent between 7 and 8 minute (filled with a yellow color) was collected together. A gradient elution method was applied: a linear gradient

of 10%−90% acetonitrile over 20 minute at a flow rate of 3 mL·min^{-1}. (B) NaCl XRD standard card and XRD pattern of 4-APBA before and after desalination. NaCl was all removed from 4-APBA sample, and a weak and broad reflection peak at $2\theta=19.2^{\circ}$ appeared in the XRD spectrum of 4-APBA before and after desalination, suggesting that the microstructure of 4-APBA did not change during the HPLC purification.

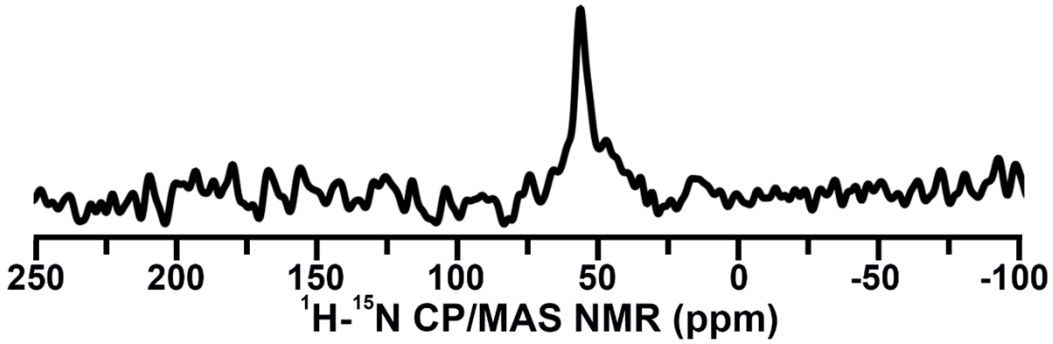

Fig. S15 ^{1}H−^{15}N CP−MAS NMR spectrum of solid 3-APBA sample.

Discussion: ^{15}N NMR spectroscopy is sensitive to the formations of dative bonds.[7,8] Except for a resonance signal of amine nitrogen at 56.3 ppm,[9] no other resonance signal was observed in the ^{1}H−^{15}N CP−MAS NMR spectrum of the solid 3-APBA sample, indicating that no B−N dative bonds were formed in 3-APBA.

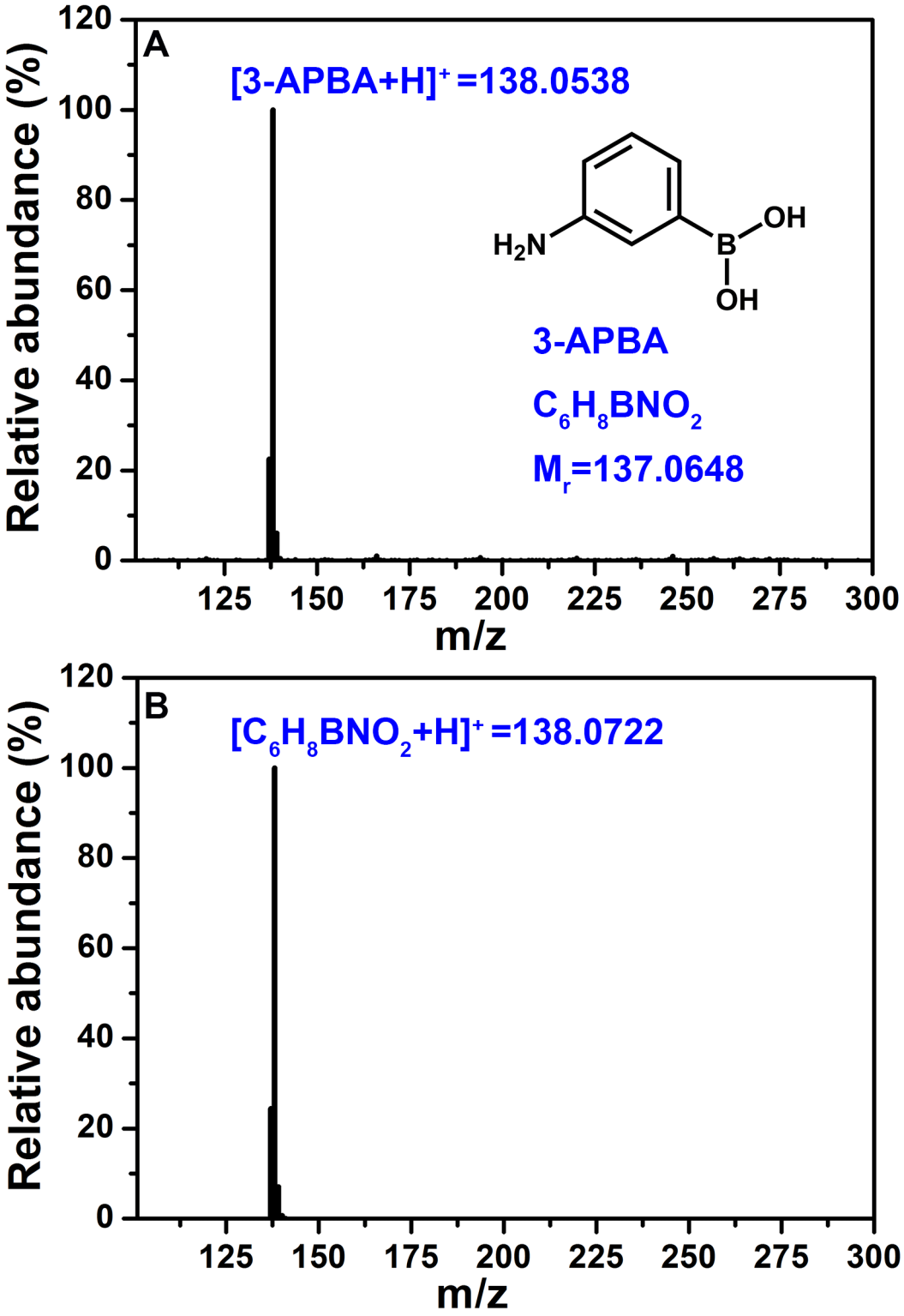

Fig. S16 Comparison of experimental (A) and simulated (B) mass spectrum of 3-APBA. **Discussion:** The isotopic distribution and molecular weight in the mass spectrum of 3-APBA were the same with these in the simulated mass spectrum of 3-APBA, which suggested that there were no boronic anhydride groups in 3-APBA.

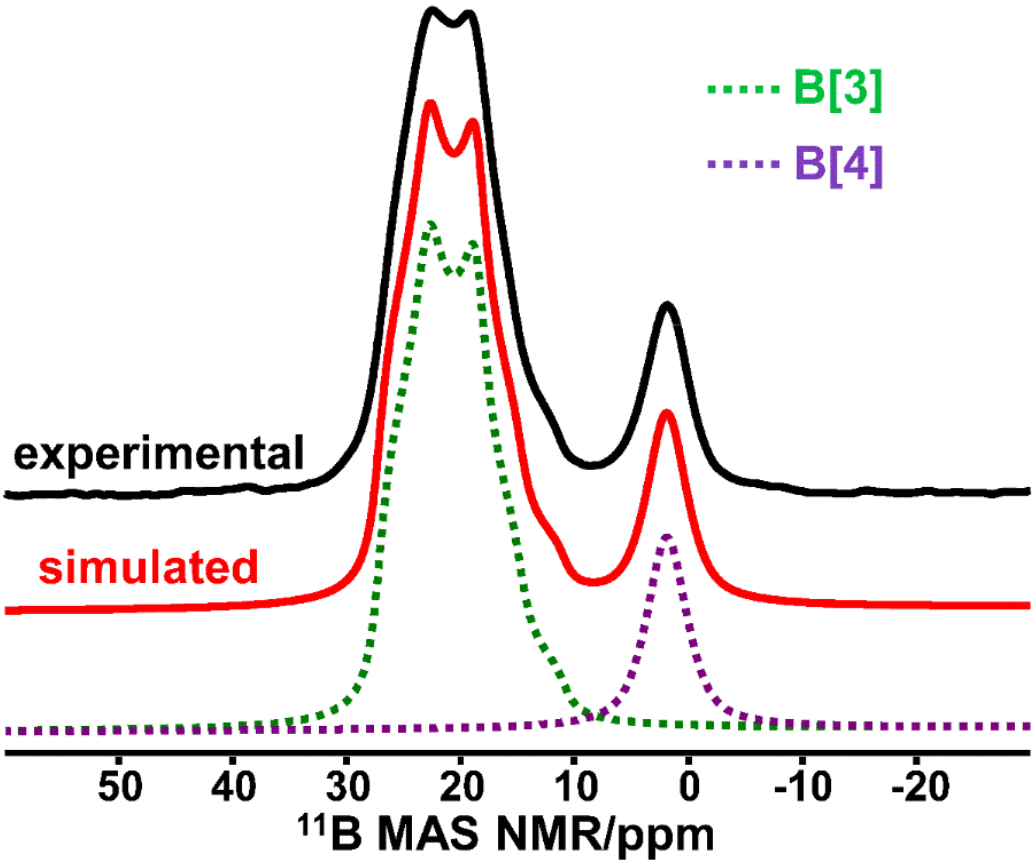

Fig. S17 ^{11}B MAS NMR experimental spectrum (black line) and the simulated line shape (red line) of solid 3-APBA sample. The simulated line shape was generated by adding together the simulated line shape of B[3] (dashed green line) and that of B[4] (dashed purple−brown line) with corresponding ratio (**Table S6**).

Discussion: Both B[3] and B[4] signal were observed in the ^{11}B MAS NMR spectrum of solid 3-APBA sample, which accounted for 83.3% and 16.7%, respectively. The B[4] signal was located at 1.9 ppm, which indicated that there existed OH^- coordinated with B in the solid 3-APBA sample.[10-12] The ^{1}H NMR spectrum of 3-APBA in DMSO−d_6 (**Fig. S19B**) showed that the number of hydrogen atoms belonging to −OH was more than that belonging to $-NH_2$ further supporting the existence of OH^- coordinated with B.

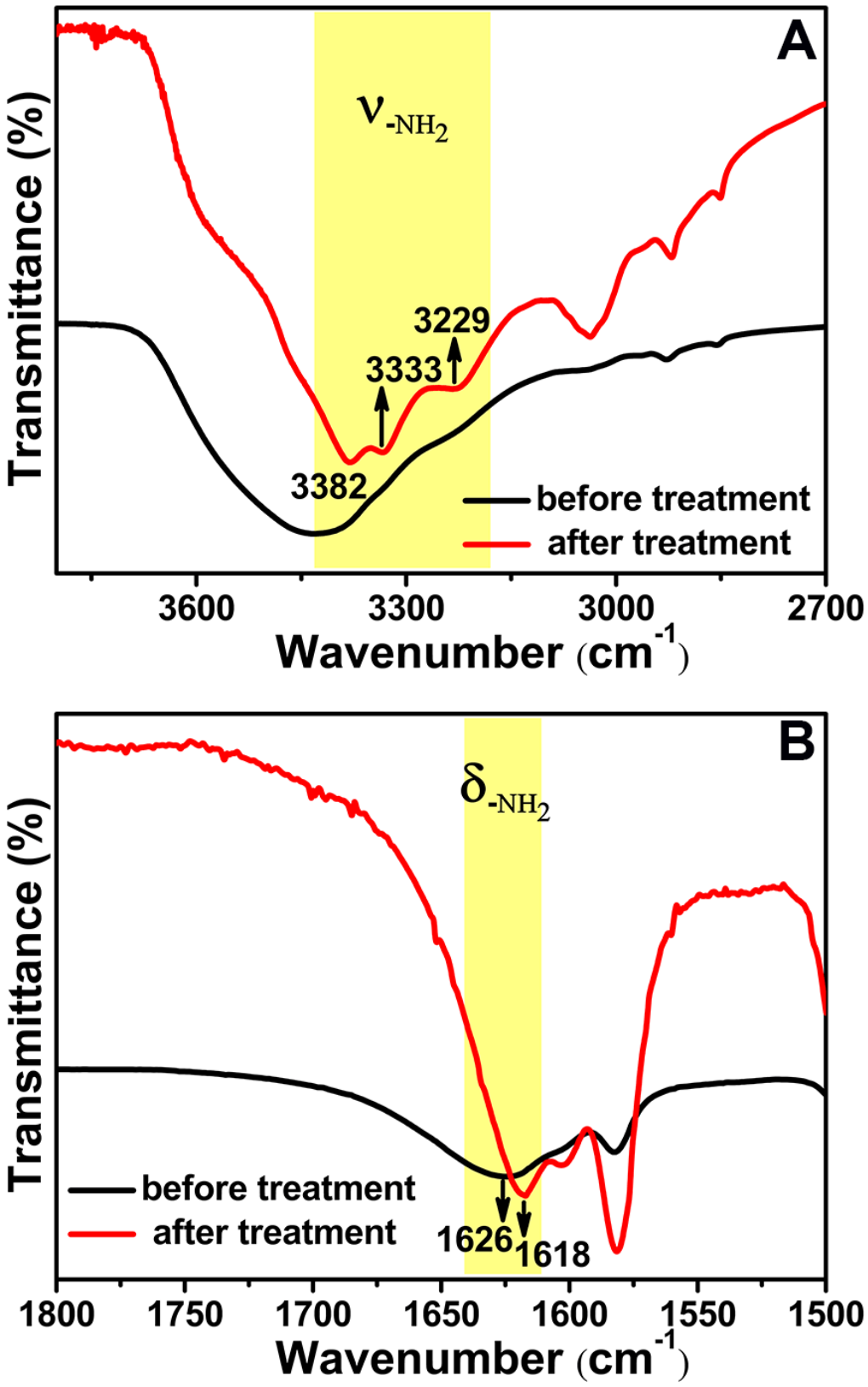

Fig. S18 FT−IR spectra of 3-APBA before and after treatment in boiling water. (A) 3800–2700 cm^{-1} range; (B) 1800–1500 cm^{-1} range. Treatment of 3-APBA in boiling water was as following: 3-APBA aqueous solution was incubated at 95 °C for 3 h, and

then the hot 3-APBA aqueous solution was frozen by liquid nitrogen. The frozen 3-APBA aqueous solution was lyophilized to get 3-APBA powder.

Discussion: In the FT−IR spectrum of 3-APBA (black line), the $\nu(-NH_2)$ was buried in the ν (−OH). After treatment in boiling water (red line), the ν ($-NH_2$) appeared and $\delta(-NH_2)$ shifted from 1626 cm^{-1} to 1618 cm^{-1} in the FT−IR spectrum of 3-APBA. The above results suggested that there existed hydrogen bonds between $-NH_2$ and −OH in 3-APBA. The hydrogen bonds broadened the bandwidth of $\nu(-NH_2)$ and made $\nu(-NH_2)$ buried in the ν(−OH).[13] After treatment in boiling water, some hydrogen bonds broke, thus $\nu(-NH_2)$ appeared and $\delta(-NH_2)$ shifted.

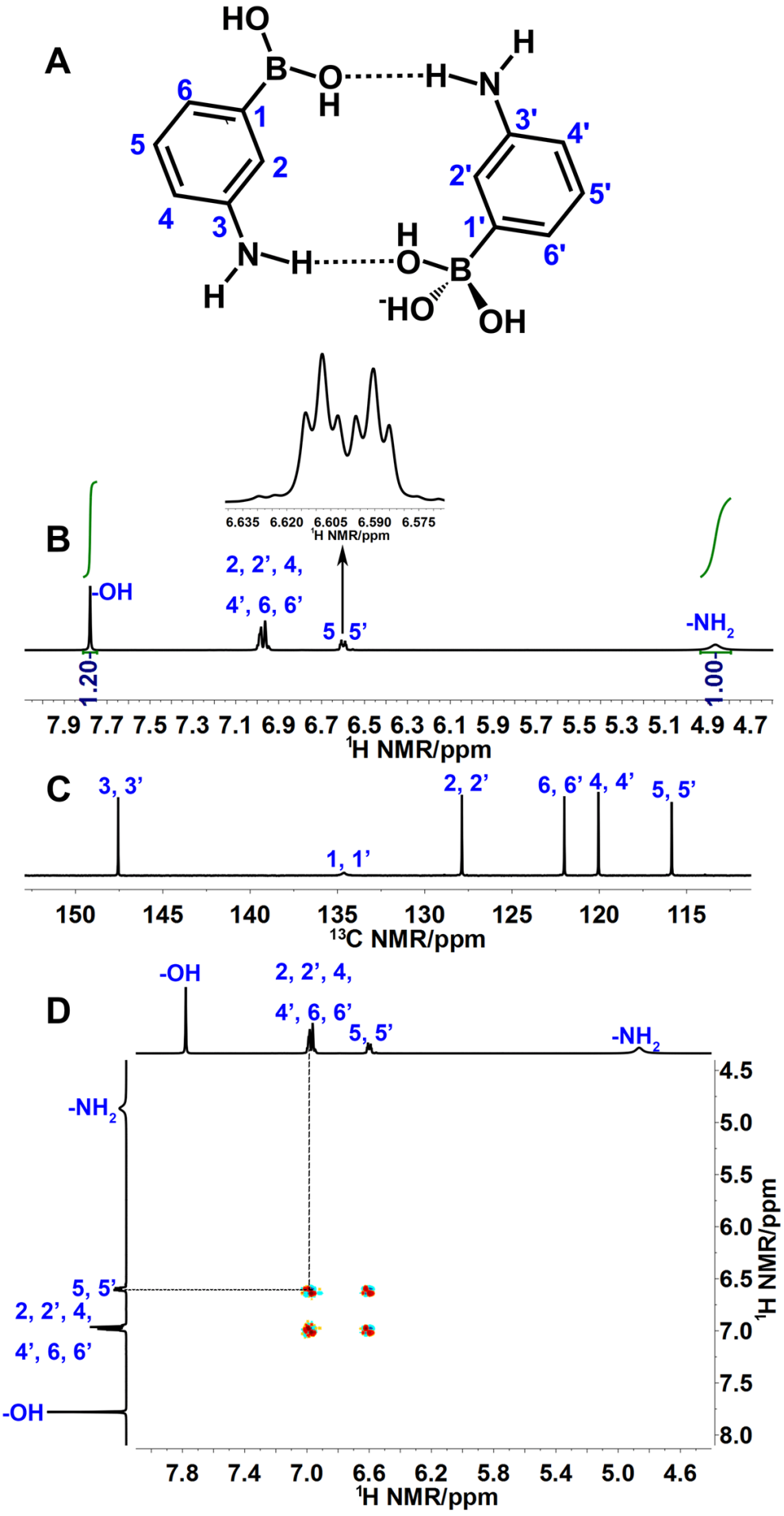
A
HO
B
O
H
H
N
H
6
1
5
2
3'
4'
2'
5'
4
3
1'
6'
N
H
H
O
B
HO
OH
B
6.635 6.620 6.605 6.590 6.575
¹H NMR/ppm
2, 2', 4,
4', 6, 6'
-OH
5 5'
-NH2
1.20
1.00
7.9 7.7 7.5 7.3 7.1 6.9 6.7 6.5 6.3 6.1 5.9 5.7 5.5 5.3 5.1 4.9 4.7
¹H NMR/ppm
C
3, 3'
2, 2'
6, 6'
4, 4'
5, 5'
1, 1'
150 145 140 135 130 125 120 115
¹³C NMR/ppm
D
-OH
2, 2', 4,
4', 6, 6'
5, 5'
-NH2
-NH2
5, 5'
2, 2', 4,
4', 6, 6'
-OH
4.5
5.0
5.5
6.0
6.5
7.0
7.5
8.0
¹H NMR/ppm
7.8 7.4 7.0 6.6 6.2 5.8 5.4 5.0 4.6
¹H NMR/ppm

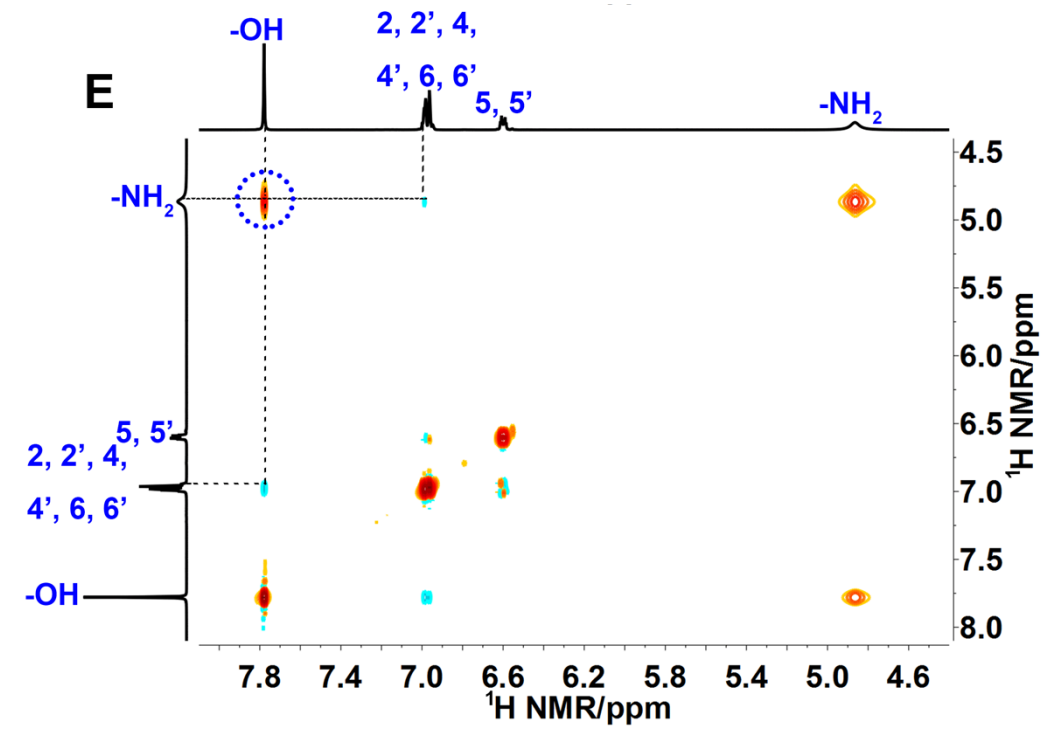
E
-OH
2, 2', 4,
4', 6, 6'
5, 5'
-NH2
-NH2
5, 5'
2, 2', 4,
4', 6, 6'
-OH
4.5
5.0
5.5
6.0
6.5
7.0
7.5
8.0
1H NMR/ppm
7.8
7.4
7.0
6.6
6.2
5.8
5.4
5.0
4.6
1H NMR/ppm

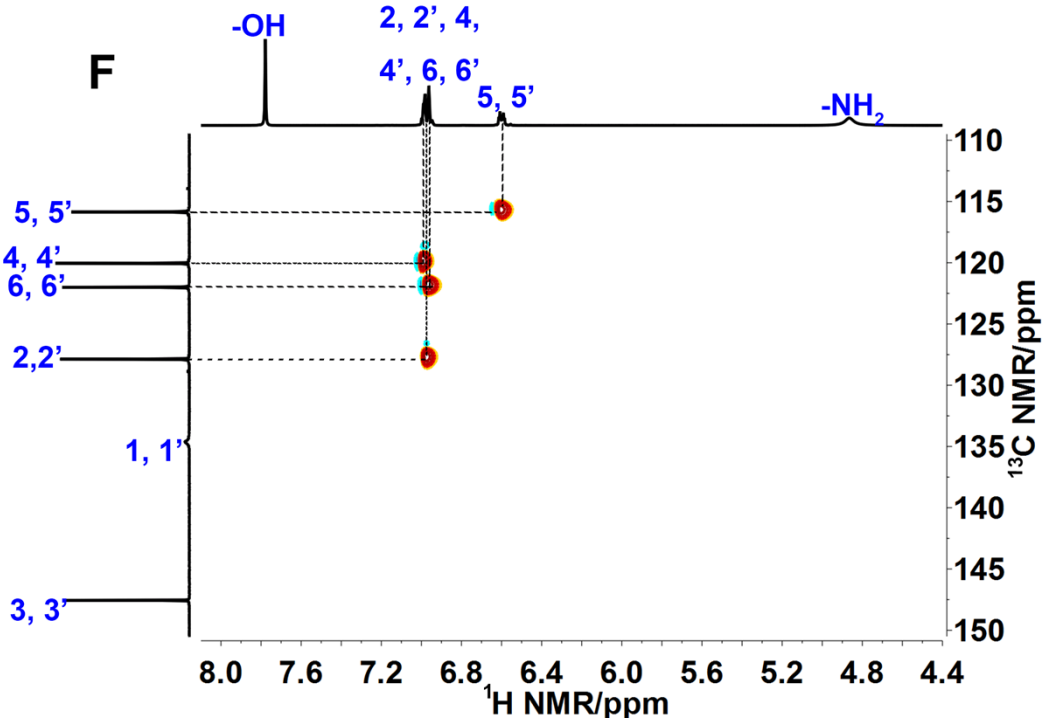
F
-OH
2, 2', 4,
4', 6, 6'
5, 5'
-NH2
5, 5'
4, 4'
6, 6'
2,2'
1, 1'
3, 3'
110
115
120
125
130
135
140
145
150
13C NMR/ppm
8.0
7.6
7.2
6.8
6.4
6.0
5.6
5.2
4.8
4.4
1H NMR/ppm

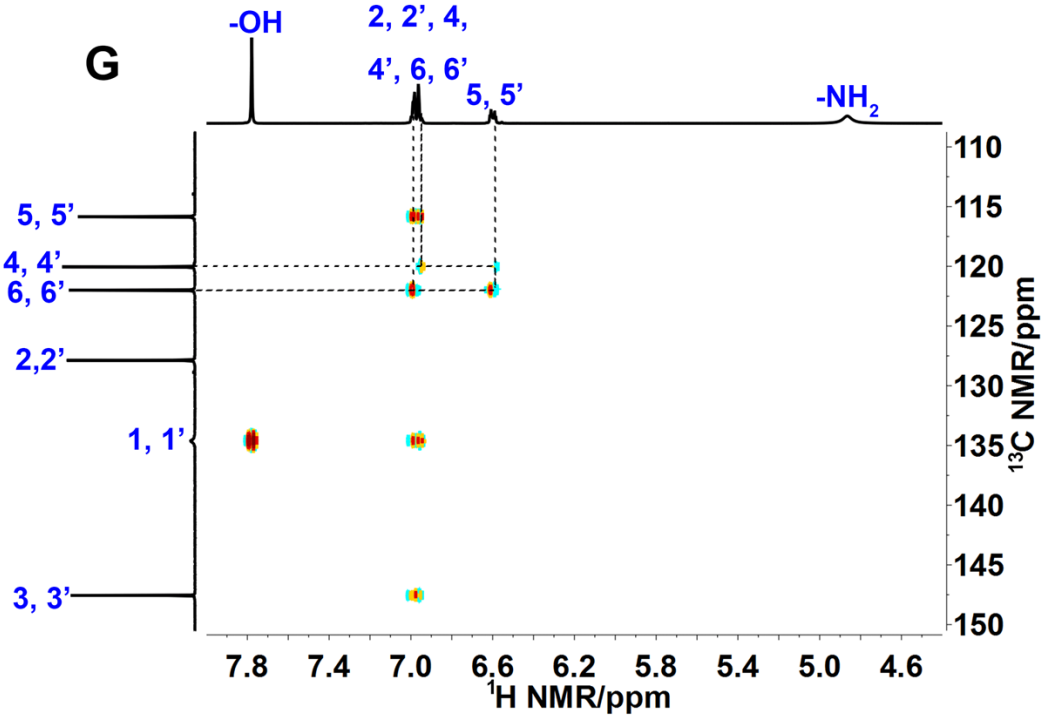

Fig. S19 Possible chemical structure of 3-APBA dimer (A) and ^{1}H (B), ^{13}C (C), ^{1}H–^{1}H COSY (D), ^{1}H–^{1}H NOESY (E), ^{1}H–^{13}C HSQC (F), ^{1}H–^{13}C HMBC (G) NMR spectra of 3-APBA dissolved in DMSO−d_6 at 20 °C. Concentration: 40 mg·mL^{-1}.

Discussion: In the NOESY spectrum of 3-APBA in DMSO−d_6, there appeared a cross peak between the H signal of −OH and that of −NH_2 (framed in a circle with dashed blue lines), further supporting that hydrogen bonds between −NH_2 and −OH existed in 3-APBA. In the fluorescence spectrum, the emission peak position of 3-APBA in water was almost identical to that of 2-APBA dimer in water (**Fig. S10A**, $\lambda_{em\ (3\text{-APBA})}$=375 nm; $\lambda_{em\ (2\text{-APBA dimer})}$=376 nm), while their maximum excitation wavelengths were also close ($\lambda_{ex\ (3\text{-APBA})}$=295 nm; $\lambda_{ex\ (2\text{-APBA dimer})}$=300 nm). Based on these facts, we reasonably presumed that 3-APBA also existed in a dimeric form that two 3-APBA molecules were connected by N−H…O interactions (**Fig. S19A**). ^{1}H and ^{13}C NMR signals of 3-APBA in DMSO−d_6 solution were assigned based on the ^{1}H–^{1}H COSY, ^{1}H–^{1}H NOESY, ^{1}H–^{13}C HSQC and ^{1}H–^{13}C HMBC NMR spectra.

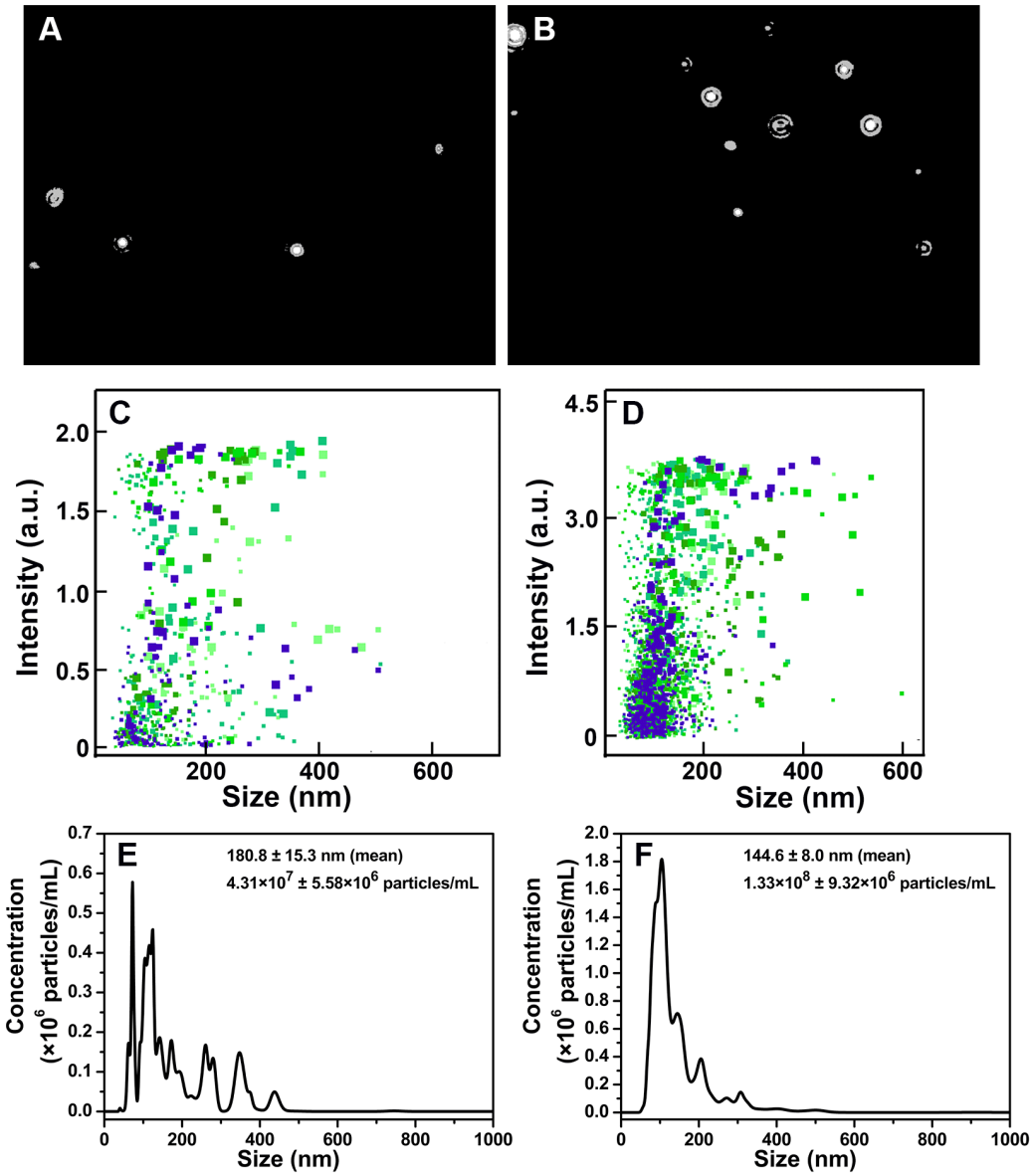

Fig. S20 A typical particle image in a 3-APBA aqueous solution with a concentration of 5.0×10^{-5} mol L^{-1} (A) or 2.0×10^{-3} mol L^{-1} (B). Size distribution graphs of 3-APBA aqueous solution with the concentration of 5.0×10^{-5} mol L^{-1} (C and E) or 2.0×10^{-3} mol L^{-1} (D and F). C and D: intensity versus size, a dot represents a particle. E and F: averaged FTLA (finite track length adjustments) concentration versus size. The above results revealed that 3-APBA existed in the form of aggregates in water, and more aggregates were formed when the concentration of 3-APBA increased.

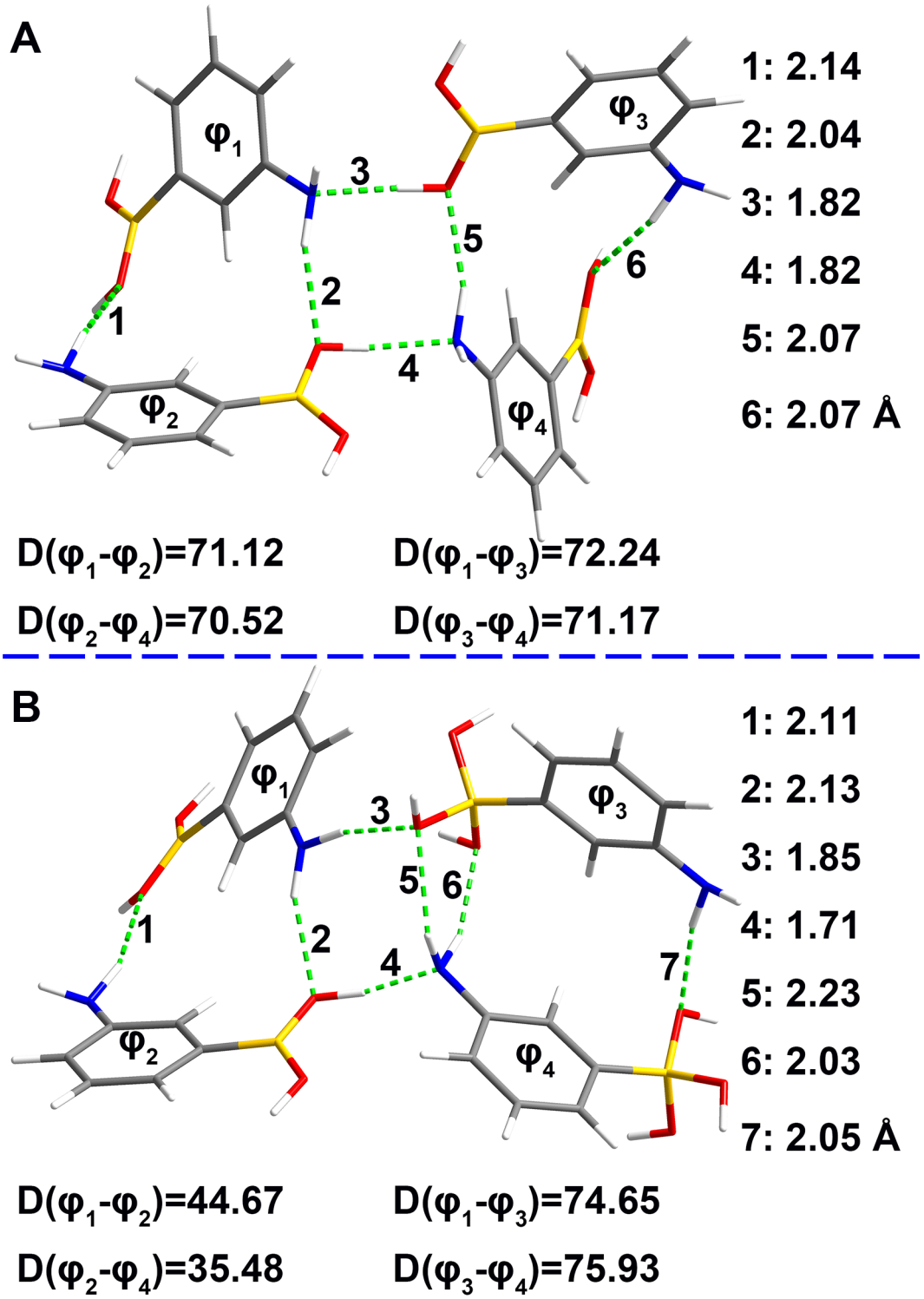

Fig. S21 DFT−optimized geometry of two connected 3-APBA dimers. (A) Two connected 3-APBA dimers containing only B[3], (B) Two connected 3-APBA dimers containing both B[3] and B[4].

Discussion: The aggregated structure of 3-APBA, which was simplified to two 3-APBA dimers, was optimized by using DFT calculations. Since the ratio of B[3] and

B[4] in 3-APBA was about 5:1 (**Table S6**), the geometries of two kinds of two connected 3-APBA dimers, one containing only B[3] (**Fig. S21A**) and the other containing both B[3] and B[4] (**Fig. S21B**), were calculated. The hydrogen bonds between boronic acid groups and amines in the 3-APBA aggregate, which precluded the reaction of 3-APBA with HBQ, were calculated to be in the length of 1.7~2.2 Å. The dihedral angles between phenyl planes ($D(\varphi_i-\varphi_j)$) in the 3-APBA aggregate ranged from 44° to 76°, which were unfavorable for the formation of ordered structure.

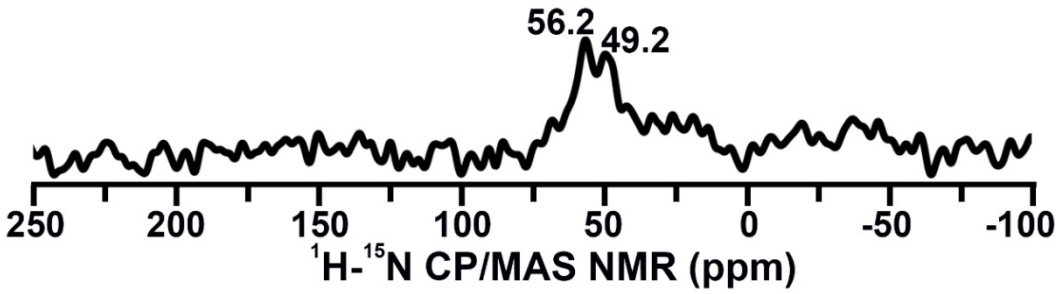

Fig. S22 ^{1}H−^{15}N CP−MAS NMR spectrum of solid 4-APBA sample.

Discussion: As shown in **Table S7,** the ratio of B[3] to B[4] in 4-APBA was about 1:1.2. Since the peak at 56.2 ppm in the ^{1}H−^{15}N CP−MAS NMR spectrum of solid 4-APBA sample **(Fig. S22**) belonged to the resonance signal of amine nitrogen in 4-APBA with B[3], the peak at 49.2 ppm could be reasonably ascribed to the resonance signal of amine nitrogen in 4-APBA with B[4]. ^{15}N NMR spectroscopy is sensitive to the formations of dative bonds. For example, Yuya *et al*. reported that 94 ppm variance of nitrogen resonance signal happened when B−N dative bonds were formed.[8] However, except for the resonance signals of amine nitrogen at 56.2 and 49.2 ppm, no other resonance signals were observed in the ^{1}H−^{15}N CP−MAS NMR spectrum of solid 4-APBA sample (**Fig. S22**)**,** indicating that no B−N dative bonds were formed in 4-APBA.

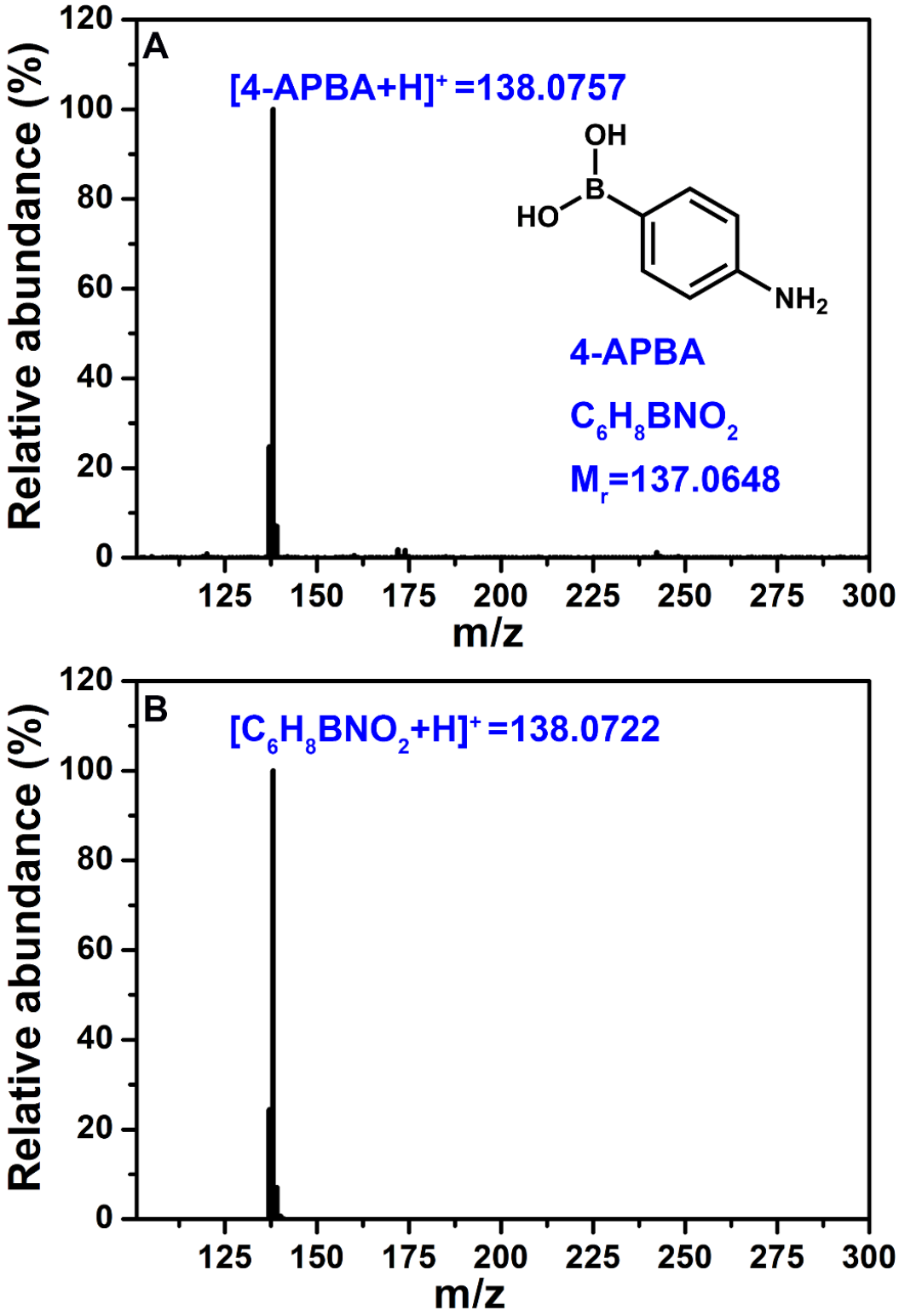

Fig. S23 Comparison of experimental (A) and simulated (B) mass spectrum of 4-APBA.

Discussion: The isotopic distribution and molecular weight in the mass spectrum of 4-APBA were the same with these in the simulated mass spectrum of 4-APBA, which suggested that there were no boronic anhydride groups in 4-APBA.

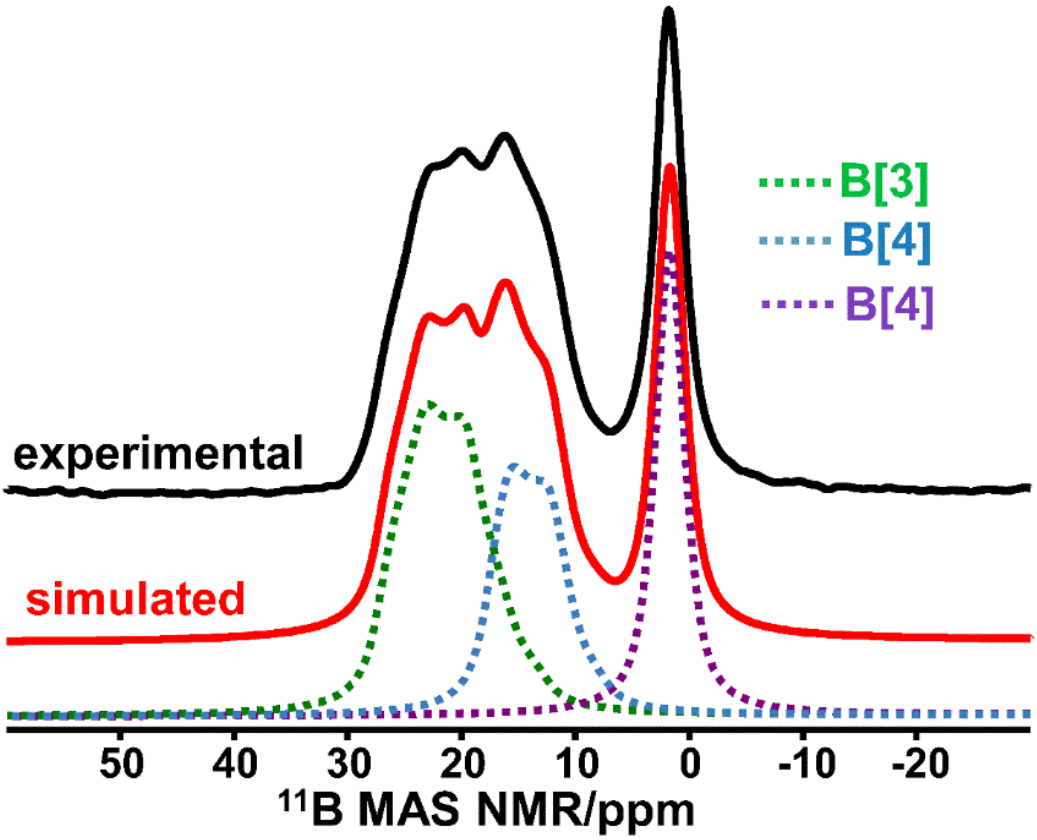

Fig. S24 ^{11}B MAS NMR experimental spectrum (black line) and the simulated line shape (red line) of solid 4-APBA sample. The simulated line shape was generated by adding together the simulated line shape of B[3] (dashed green line) and these of B[4] (dashed blue and purple−brown line) with corresponding ratios (**Table S7**).

Discussion: Both B[3] and B[4] signal were observed in the ^{11}B MAS NMR spectrum of the solid 4-APBA sample, which accounted for 45.5% and 54.5%, respectively (**Table S7**).The B[4] signal located at around 18.5 ppm resulted from the coordinate interaction between water and B, and B[4] signal located at around 2 ppm indicated that there existed OH^- coordinated with B in the solid 4-APBA sample.[10-12] The ^{1}H NMR spectrum of 4-APBA in DMSO−d_6 showed that the number of hydrogen atoms belonging to −OH was more than that belonging to $-NH_2$ further supporting the existence of OH^- and water coordinated with B (**Fig. S25**B). Thus three species, i.e. 4-APBA, 4-APBA coordinated with water and 4-APBA coordinated with OH^-, should exist in the solid 4-APBA sample.

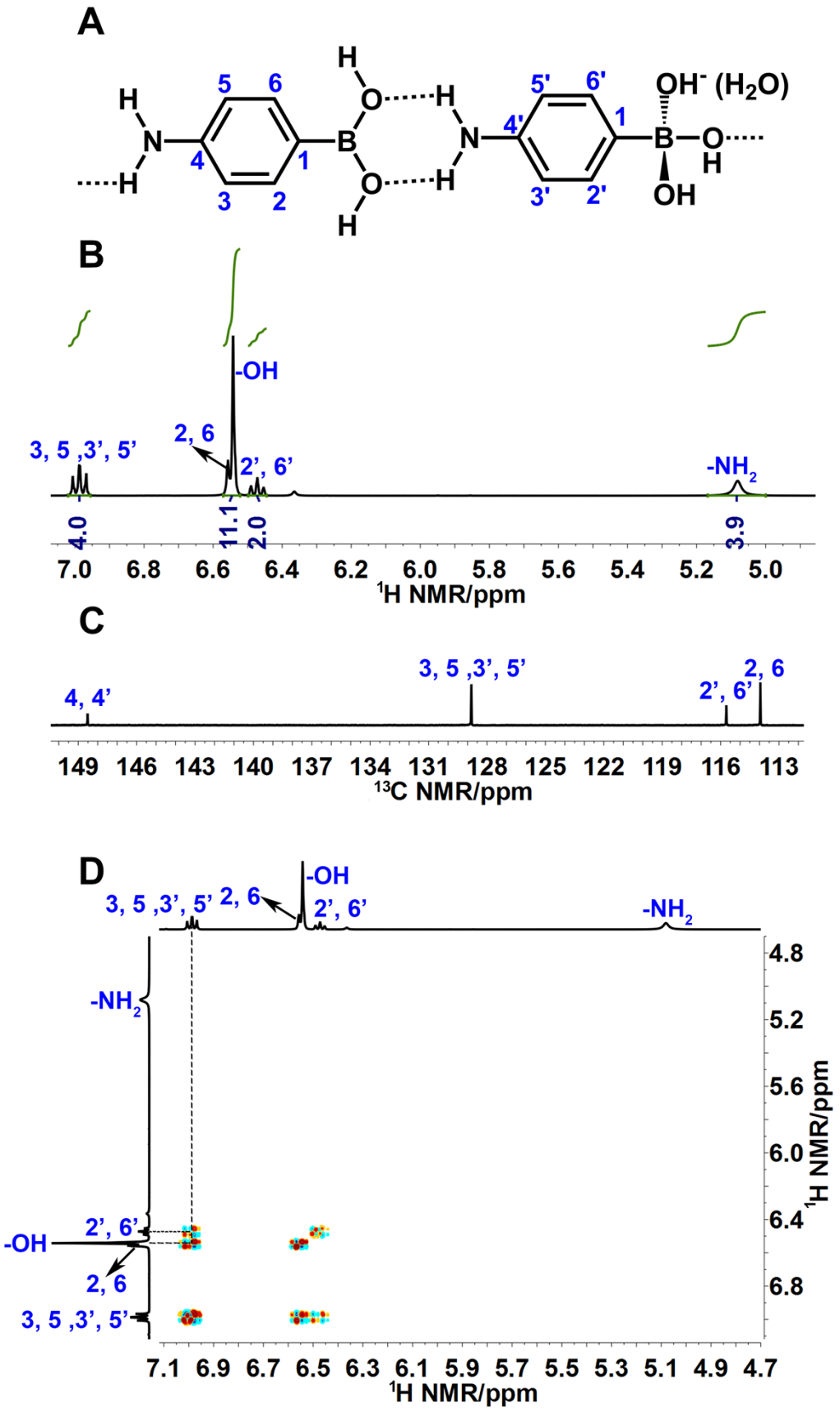
A
B
C
D
-OH
2, 6
2', 6'
3, 5 ,3', 5'
-NH2
4.0
11.1
2.0
3.9
7.0 6.8 6.6 6.4 6.2 6.0 5.8 5.6 5.4 5.2 5.0
1H NMR/ppm
4, 4'
149 146 143 140 137 134 131 128 125 122 119 116 113
13C NMR/ppm
7.1 6.9 6.7 6.5 6.3 6.1 5.9 5.7 5.5 5.3 5.1 4.9 4.7
4.8 5.2 5.6 6.0 6.4 6.8

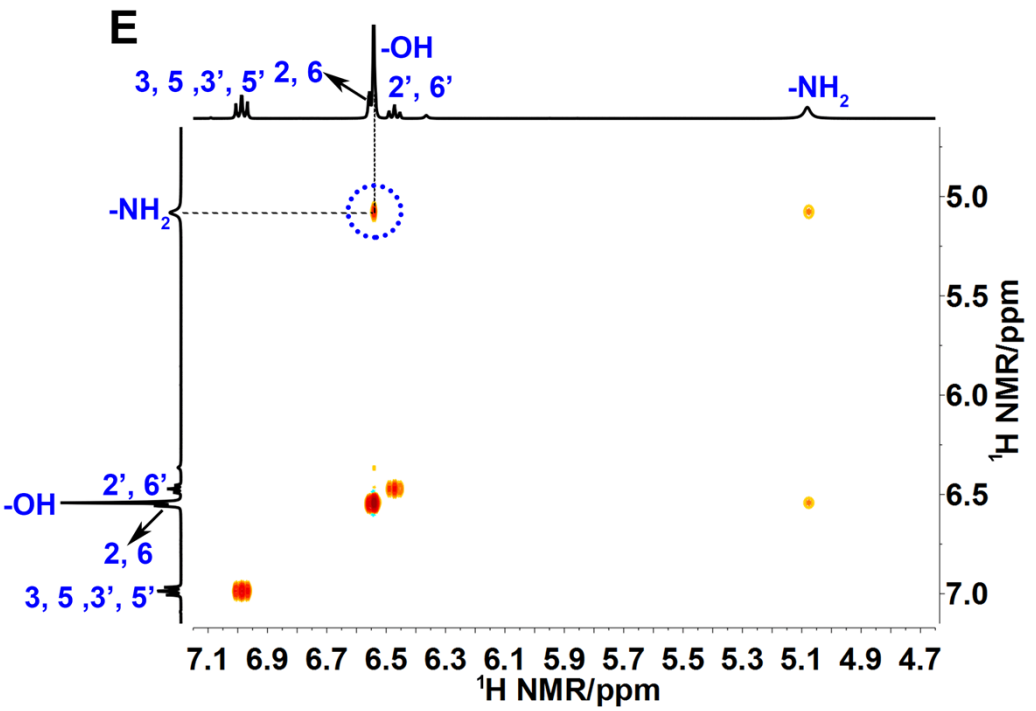
E
-OH
3, 5 ,3', 5' 2, 6
2', 6'
-NH2
-NH2
2', 6'
-OH
2, 6
3, 5 ,3', 5'
5.0
5.5
6.0
6.5
7.0
1H NMR/ppm
7.1 6.9 6.7 6.5 6.3 6.1 5.9 5.7 5.5 5.3 5.1 4.9 4.7
1H NMR/ppm

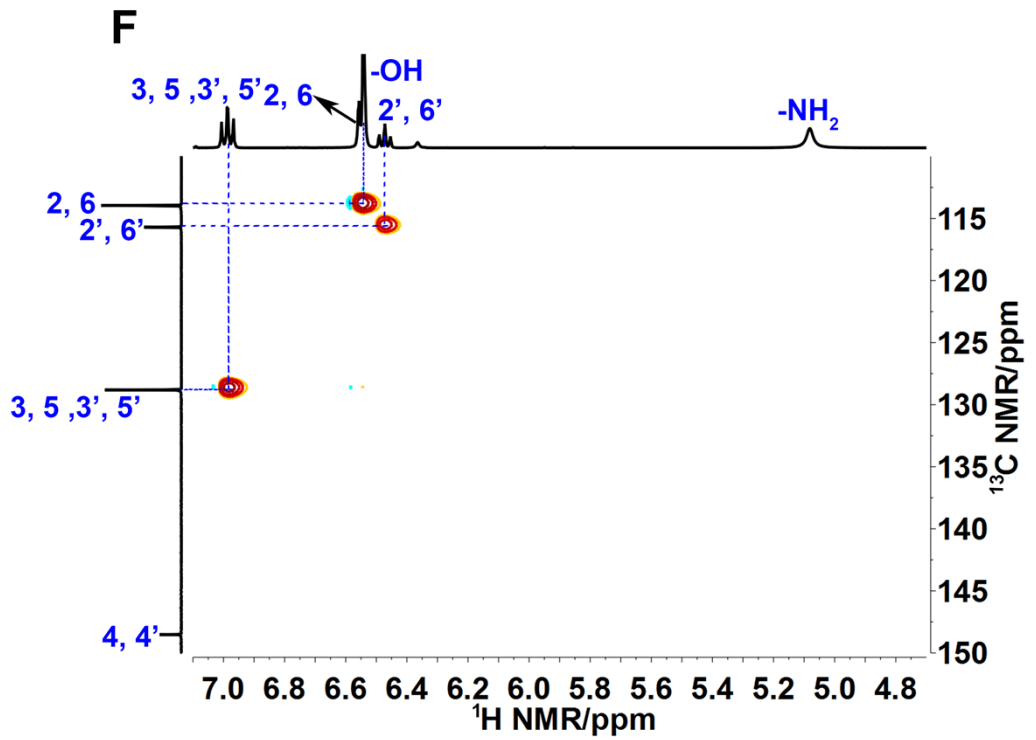
F
-OH
3, 5 ,3', 5'2, 6
2', 6'
-NH2
2, 6
2', 6'
3, 5 ,3', 5'
4, 4'
115
120
125
130
135
140
145
150
13C NMR/ppm
7.0 6.8 6.6 6.4 6.2 6.0 5.8 5.6 5.4 5.2 5.0 4.8
1H NMR/ppm

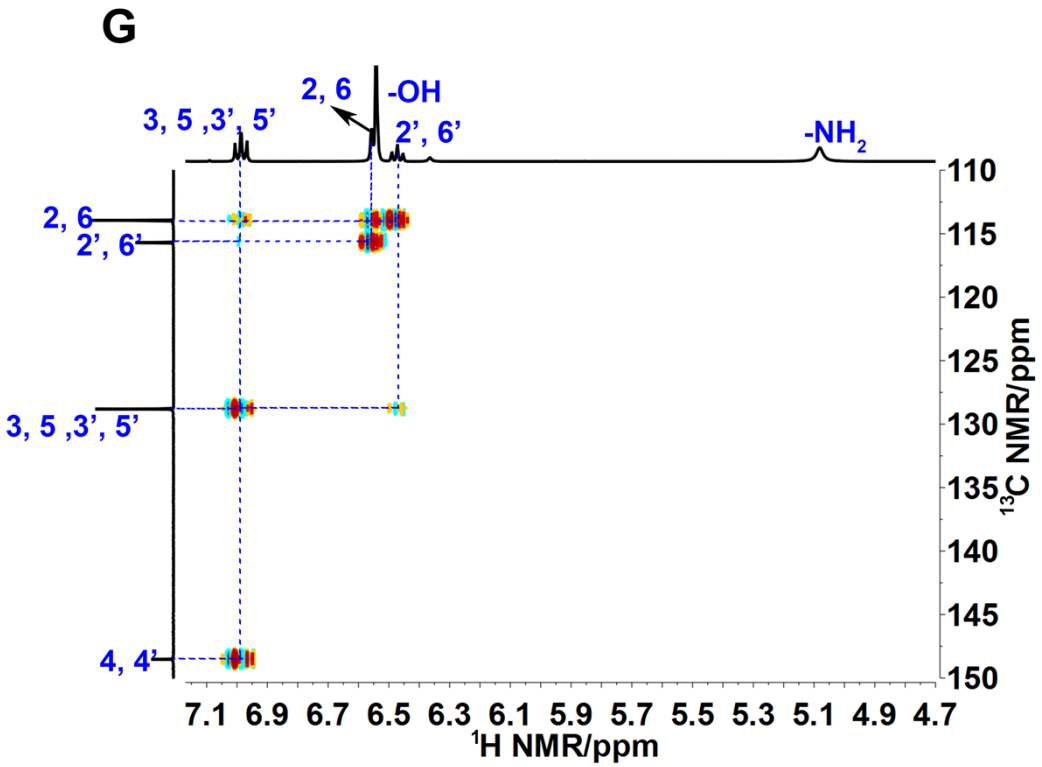

Fig. S25 Possible chemical structure of 4-APBA dimer (A) and ^{1}H (B), ^{13}C (C), ^{1}H–^{1}H COSY (D), ^{1}H–^{1}H NOESY (E), ^{1}H–^{13}C HSQC (F), ^{1}H–^{13}C HMBC (G) NMR spectra of 4-APBA dissolved in DMSO−d_6 at 20 °C. Concentration: 40 mg·mL^{-1}.

Discussion: In the NOESY spectrum of 4-APBA in DMSO−d_6, there appeared a cross peak between the H signal of −OH and that of −NH_2 (**Fig. S25E**, framed in a circle with dashed blue lines), supporting that hydrogen bonds between −NH_2 and −OH existed in 4-APBA (**Fig. S25A**). ^{1}H and ^{13}C NMR signals of 4-APBA in DMSO−d_6 were assigned based on the ^{1}H–^{1}H COSY, ^{1}H–^{1}H NOESY, ^{1}H–^{13}C HSQC and ^{1}H–^{13}C HMBC NMR spectrum.

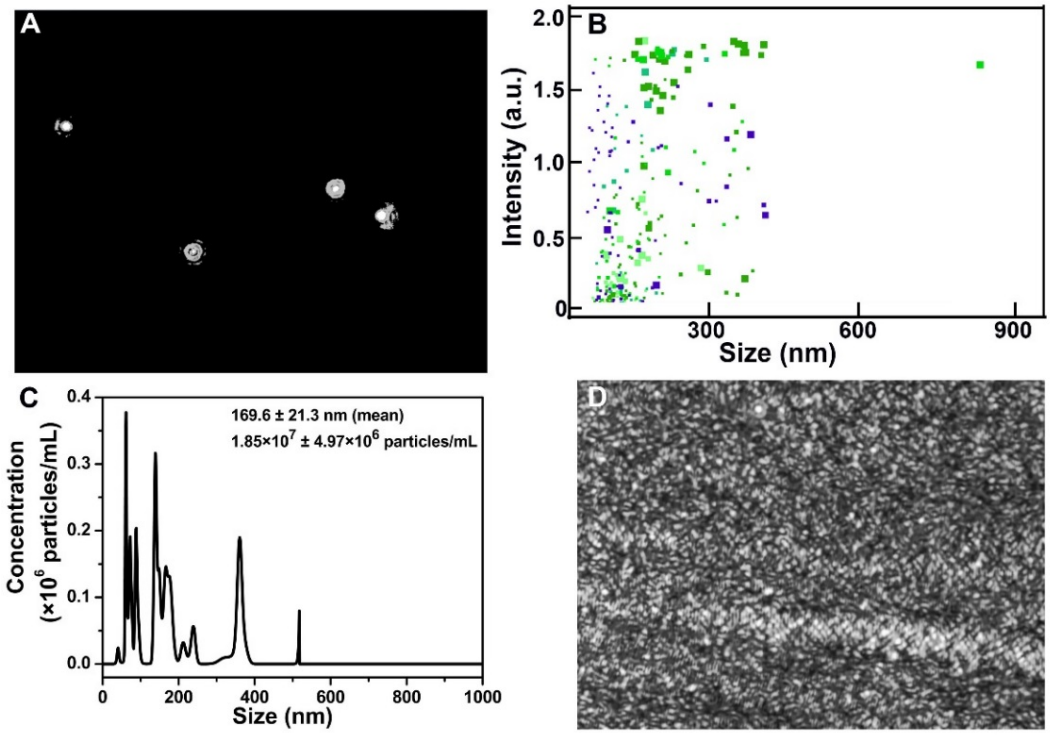

Fig. S26 (A, B, C) A typical particle image (A) and size distribution graph (B, C) of 4-APBA aqueous solution with the concentration of 5.0×10^{-5} mol L^{-1}. B: intensity versus size, a dot represents a particle. C: averaged FTLA (finite track length adjustments) concentration versus size. (D) A typical particle image in 4-APBA aqueous solution with the concentration of 2.0×10^{-3} mol L^{-1}.

Discussion: As shown in **Fig. S26A-C**, particles could be observed in the 4-APBA aqueous solution when the concentration of 4-APBA was 5.0×10^{-5} mol L^{-1}. That meant 4-APBA existed in the form of aggregate in water. Since the amine and boronic acid groups of 4-APBA are in a para arrangement, it is reasonable to presume that 4-APBA molecules are connected by hydrogen bonds to form long and flexible chains.

When the concentration of 4-APBA increased to 2.0×10^{-3} mol L^{-1}, many white spots appeared in the background of the particle image after a 4-APBA aqueous solution was injected into the measuring cell (**Fig. S26D**), which made it impossible to get the size distribution of 4-APBA aqueous solution. In a higher concentration, more 4-APBA chains could be formed. The white spots in the particle image might be the result of adsorption of 4-APBA chains in the wall of the measuring cell.

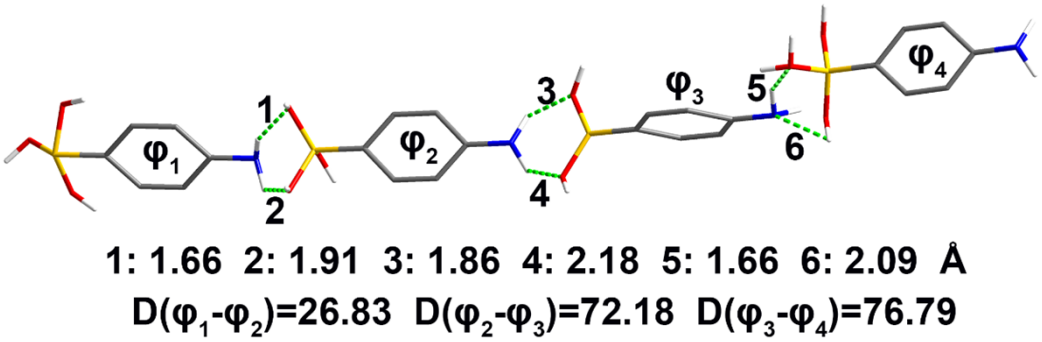

Fig. S27 DFT−optimized geometry of four connected 4-APBA.

Discussion: The geometry of 4-APBA chain simplified to four connected 4-APBA was optimized by using DFT calculations. The hydrogen bonds between boronic acid groups and amines in 4-APBA chain, which precluded the reaction of 4-APBA with HBQ, were calculated to be in the length of 1.6~2.2 Å. The dihedral angles between phenyl planes (D(φ_i−φ_j)) ranged from 27° to 77°. That meant contorted geometries were adopted in the 4-APBA chain (**Fig. S27**). The long, flexible and contorted 4-APBA chain would result in a disordered molecular packing.

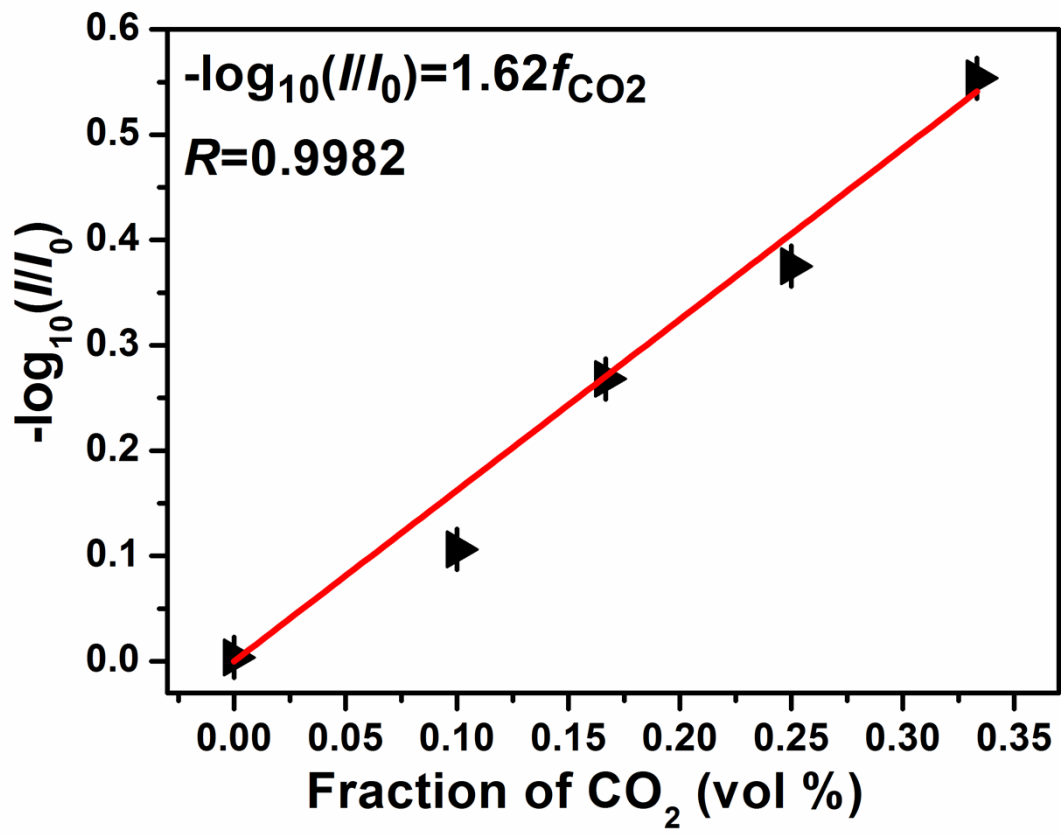

Fig. S28 Plot of $-\log_{10}(I/I_0)$ versus fraction of CO_2 (f_{CO2}) in CO_2/N_2 mixtures.

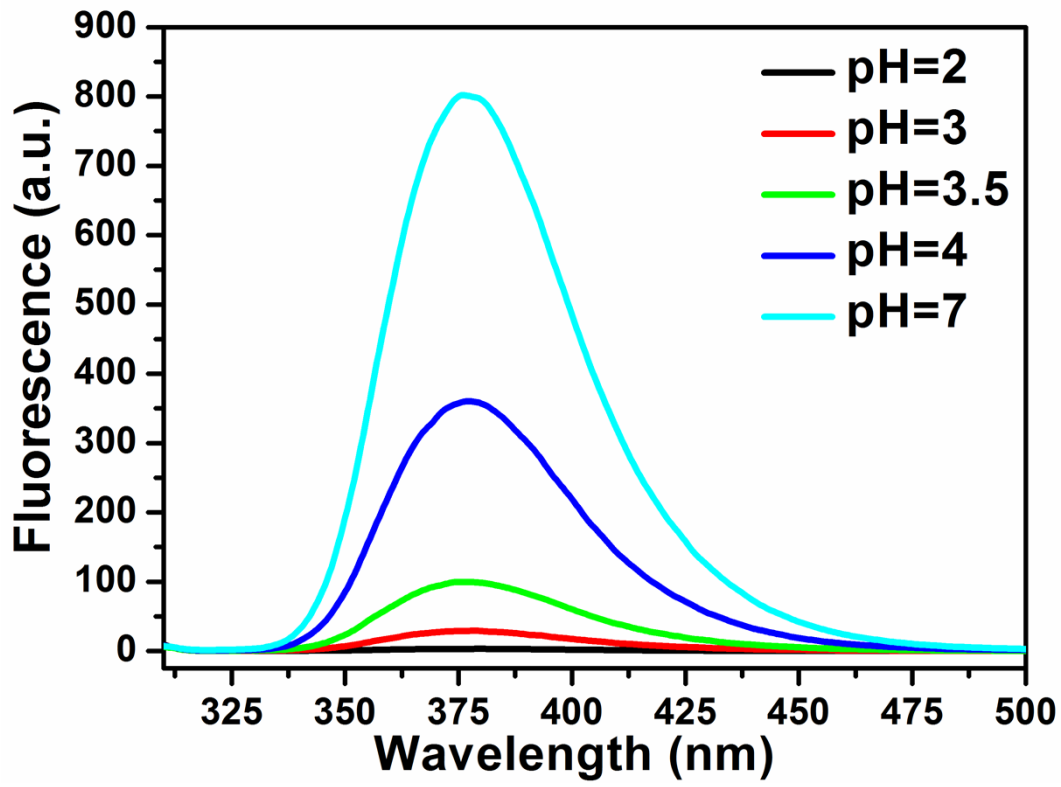

Fig. S29 Fluorescence spectra of 2-APBA dimer aqueous solutions with different pH values (5.0×10^{-5} mol·L^{-1}).

Discussion: As shown in **Fig. S29**, the fluorescence intensity of 2-APBA dimer decreased with the decreasing of pH value in the acidic solutions. Thus, the CO_2-quenching fluorescence of 2-APBA dimer could be explained to be the result of the dissolution of CO_2 in water, which reduced the pH value of the solution.

At the aid of H^+, 2-APBA dimers hydrolyze into 2-APBA monomers which was non-emissive (**Fig. S5**). Since the fluorescence of 2-APBA dimer was not completely quenched after CO_2 bubbling (Fig. 5A in the text), it was reasonable to presume that 2-APBA monomer and 2-APBA dimer coexisted in the solution upon CO_2 bubbling, which was confirmed by the results of ^{1}H and DEPT 45 ^{13}C NMR spectrum of 2-APBA in D_2O solution saturated with CO_2 (**Fig. S30**). The fluorescence of 2-APBA dimer decreased by 86% after CO_2 bubbling, which indicated most of 2-APBA dimers in D_2O solution have turned into 2-APBA monomers, remaining a small proportion of dimmers.

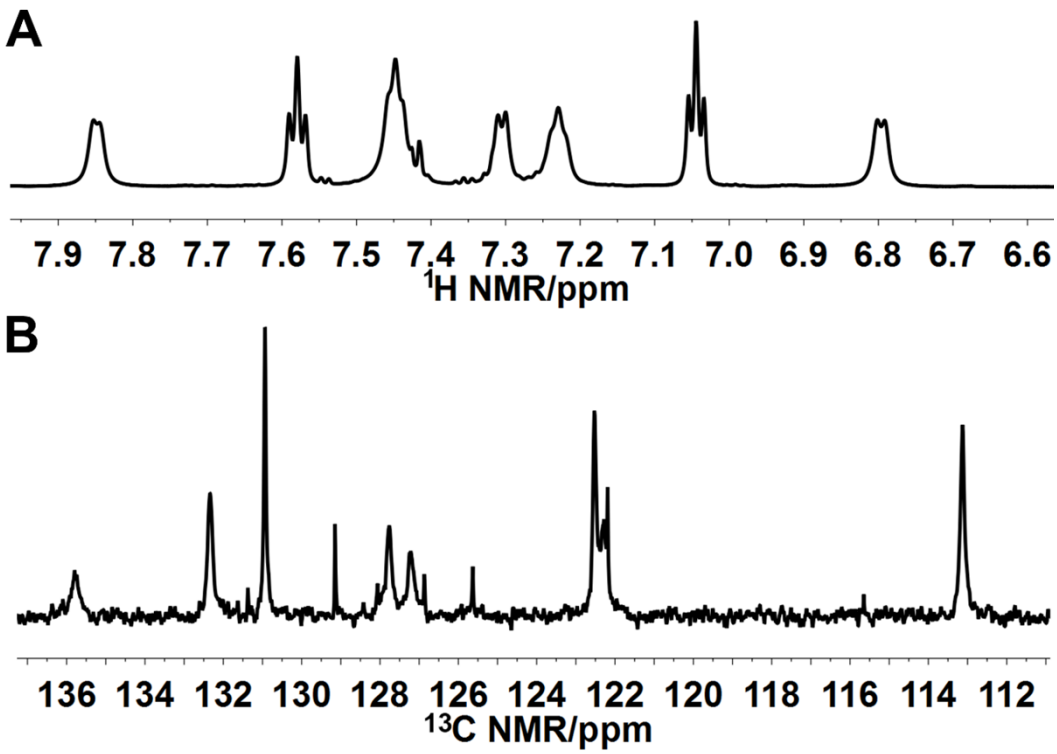

Fig. S30 ^{1}H (A) and DEPT 45 ^{13}C (B) NMR spectra of D_2O solution of 2-APBA saturated with CO_2 at 20 ^{o}C.

Discussion: 2-APBA was not readily soluble in D_2O, thus a 700 MHz NMR spectrometer and DEPT 45 pulse sequence were adopted to get a clear ^{13}C NMR spectrum of D_2O solution of 2-APBA saturated with CO_2. The numbers of ^{1}H and ^{13}C signals in **Fig. S30** were much more than these of 2-APBA monomer in hydrochloric acid solution (**Fig. S5**), which implied 2-APBA monomer and 2-APBA dimer coexisted in the D_2O solution of 2-APBA upon CO_2 bubbling.

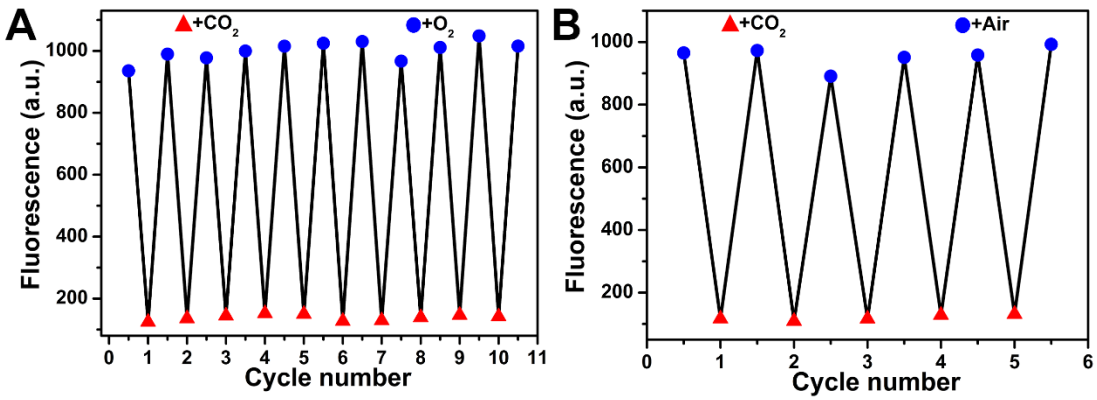

Fig. S31 Cycling experiment illustrating the variation of the fluorescent intensities of 2-APBA at 377.5 nm after alternately bubbling CO_2 and O_2 (A) or CO_2 and air (B) to an aqueous solution of 2-APBA dimer.

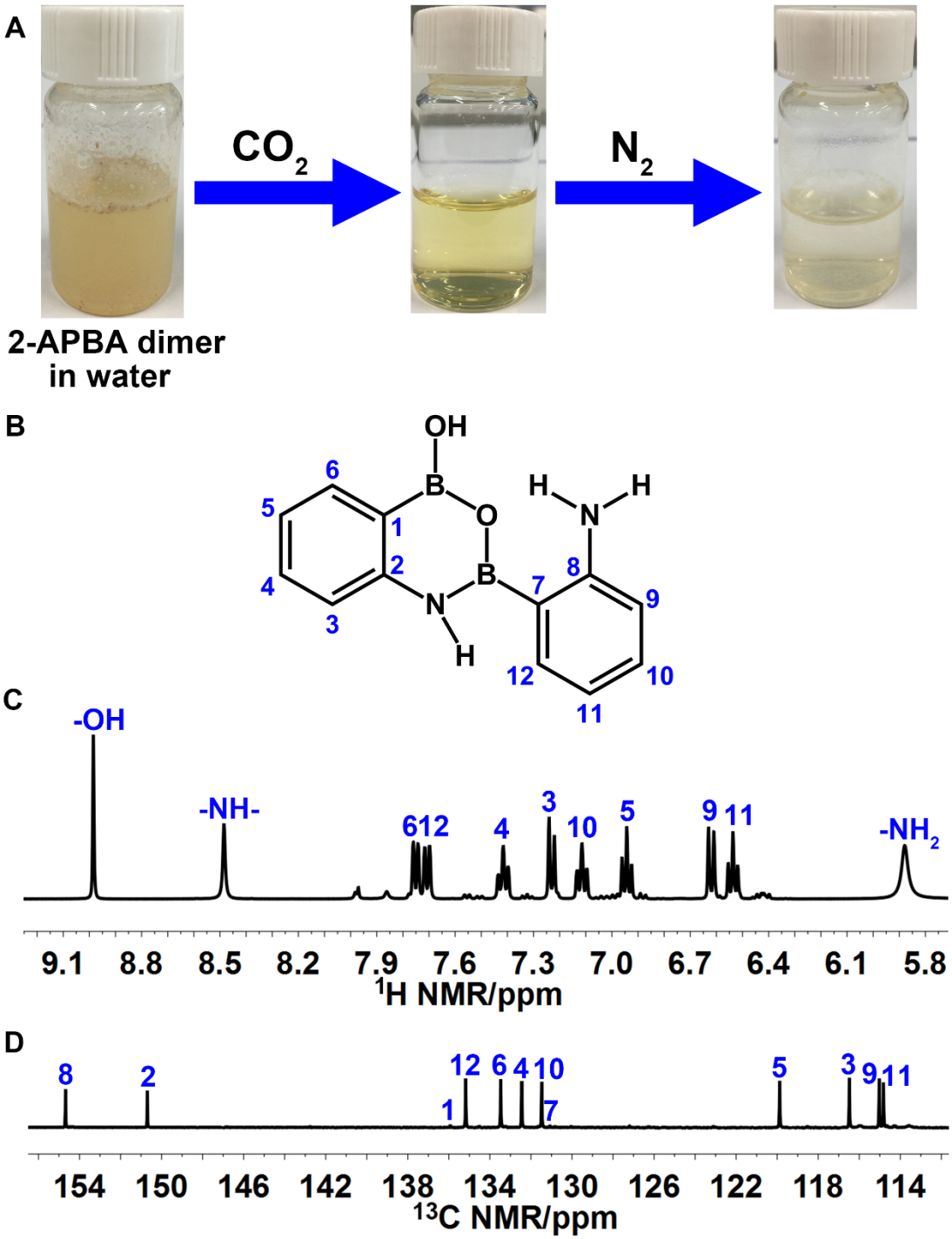

Fig. S32 (A) Photographs of 2-APBA dimer in water without any treatment (left), treated with CO_2 (middle) and then treated with N_2 (right). (B) Chemical structure of 2-APBA dimer. (C, D) ^{1}H (C) and ^{13}C (D) NMR spectra of DMSO−d_6 solution of 2-APBA dimer sample alternately treated by CO_2 and N_2. Temperature: 20 °C, Concentration: 20 mg·mL^{-1}.

Discussion: As shown in **Fig. S32A**, the turbid 2-APBA dimer aqueous dispersion became clear after CO_2 bubbling, and then sediments appeared after N_2 bubbling. The sediments were dried at room temperature, and then dissolved in DMSO−d_6 to perform ^1H and ^{13}C NMR measurement. The ^1H and ^{13}C NMR spectrum of sediments **(Fig. S32C-D)** suggested that the sediments were 2-APBA dimer **(Fig. S32B, Fig. S3).**

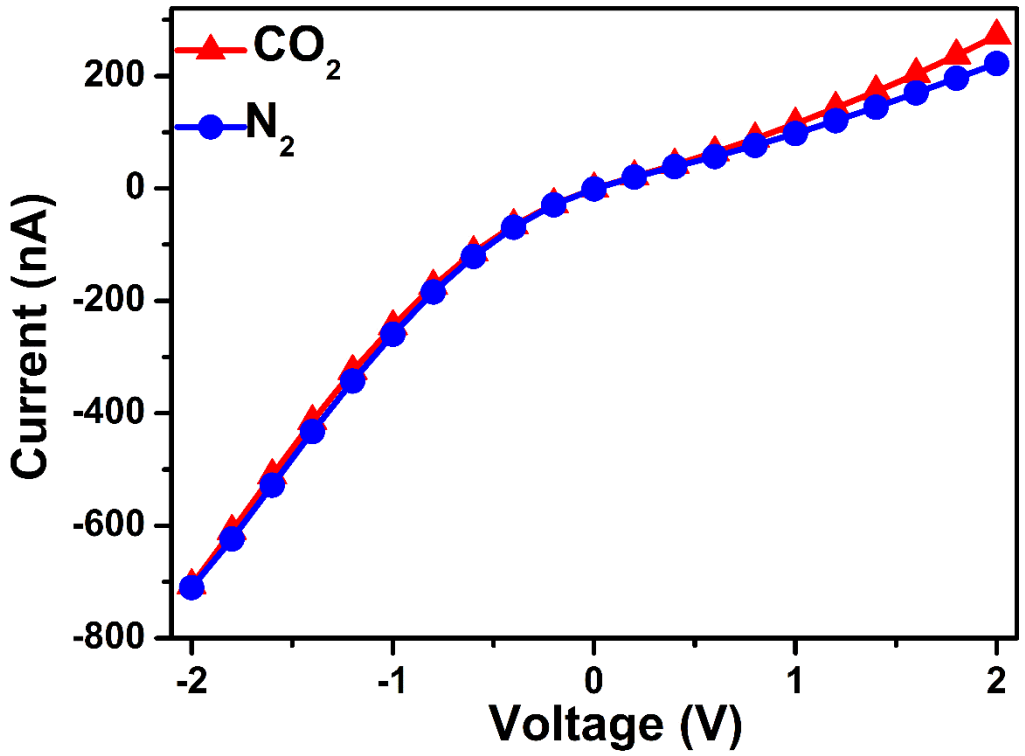

Fig. S33 Current−voltage (*I*−*V*) response recorded after CO_2 and N_2 bubbling to PET nanochannels in 0.1 mol L^{-1} KCl solution.

Tables:

Table S1 Crystal data and structure refinements for 2-APBA

Empirical formula	$C_{12}H_{12}B_2N_2O_2$
Formula weight	237.86
Temperature (K)	120(2)
Crystal size (mm^3)	0.15 x 0.15 x 0.10
Crystal system	monoclinic
Space group	P 12/n1
a (Å)	15.0331(6)
b (Å)	5.0718(3)
c (Å)	15.8131(8)
α (°)	90
β (°)	111.040(2)
γ (°)	90
V ($Å^3$)	1125.29(10)
Z	4
Density (calculated) (g/cm^3)	1.40392
F (000)	496
Theta range for data collection	2.76 to 29.99
Index ranges	−20<=h<=19, −5<=k<=6, −21<=l<=17
Reflections collected	9851
Independent reflections	2790 [R(int)=0.0499]
Final R indices [I>2sigma(I)]	R1=0.0482, wR2=0.1048
R indices (all data)	R1=0.0792, wR2=0.1204
Goodness−of−fit on F^2	1.027
Highest difference peak and deepest hole (e $Å^{-3}$)	0.284 and -0.226

Table S2 Bond lengths (Å) and angles for 2-APBA

O1−B2	1.386(2)	C11−C12-C7	117.97(15)
O1−B1	1.3867(19)	C11−C12-B2	124.14(14)
O2-B2	1.355(2)	C1−C6−B1	123.46(14)
O2-H2	0.93(3)	C5−C6−C1	116.22(15)
N2-C7	1.402(2)	C5−C6−B1	120.27(14)
N2-B1	1.415(2)	C7−C8−H8	118.0(11)
N2-H2A	0.908(19)	C9−C8−C7	119.82(15)
N1−H1A	0.8816	C9−C8−H8	122.2(11)
N1−C1	1.4119(19)	N2-C7−C12	118.49(14)
N1−H1B	0.89(2)	C8−C7−N2	120.93(14)
C12-C7	1.408(2)	C8−C7−C12	120.58(15)
C12-C11	1.400(2)	C12-C11−H11	118.5(11)
C12-B2	1.546(2)	C10−C11−C12	121.68(15)
C6−C1	1.412(2)	C10−C11−H11	119.9(11)
C6−C5	1.405(2)	N1−C1−C6	120.99(14)
C6−B1	1.563(2)	C2-C1−N1	118.15(15)
C8−C7	1.396(2)	C2-C1−C6	120.80(14)
C8−C9	1.383(2)	C6−C5−H5	118.4
C8−H8	0.991(19)	C4-C5−C6	123.14(16)
C11−C10	1.385(2)	C4-C5−H5	118.4
C11−H11	0.980(17)	C11−C10−C9	119.24(16)
C1−C2	1.396(2)	C11−C10−H10	120.7(11)
C5−H5	0.95	C9−C10−H10	120.0(11)
C5−C4	1.384(2)	C8−C9−C10	120.70(16)
C10−C9	1.392(2)	C8−C9−H9	118.9(10)
C10−H10	0.97(2)	C10−C9−H9	120.4(11)
C9−H9	0.990(19)	C1−C2-H2B	119.6

C2-H2B	0.95	C3-C2-C1	120.75(16)
C2-C3	1.381(2)	C3-C2-H2B	119.6
C3-H3	0.95	C2-C3-H3	120
C3-C4	1.386(2)	C2-C3-C4	119.99(16)
C4-H4	0.95	C4-C3-H3	120
B2-O1−B1	123.08(13)	C5−C4-C3	119.07(15)
B2-O2-H2	114.0(14)	C5−C4-H4	120.5
C7−N2-B1	124.62(14)	C3-C4-H4	120.5
C7−N2-H2A	114.2(12)	O1−B2-C12	118.16(14)
B1−N2-H2A	121.1(12)	O2-B2-O1	120.09(15)
H1A−N1−H1B	113.6	O2-B2-C12	121.73(15)
C1−N1−H1A	109.7	O1−B1−N2	117.72(15)
C1−N1−H1B	112.8(13)	O1−B1−C6	119.84(15)
C7−C12-B2	117.85(14)	N2-B1−C6	122.44(14)

Table S3 Hydrogen bond data for 2-APBA

D−H...A	d(D−H)	d(H...A)	d(D...A)	<(DHA)
N1−H1B...O1	0.89 (2)	2.087 (20)	2.745 (2)	130 (2)
O2-H2...N1^{i}	0.93 (3)	1.965 (26)	2.891 (2)	176 (2)
C10−H10...O2^{ii}	0.97(2)	2.859 (21)	3.402 (2)	117 (2)

Symmetry codes: (i) 1−*x*, 1−*y*, 1−*z*; (ii) −1+*x*, *y*, *z*.

Table S4 Photophysical parameters of 3-APBA in THF, water and the solid state

	Φ_F (absolute)	τ (ns)	<τ> (ns)	k_F (s^{-1})	k_{nr} (s^{-1})	k_F/k_{nr}
In THF	21.2%	4.87	/	4.35×10^7	1.62×10^8	0.27
In water	20.1%	1.10	/	1.83×10^8	7.27×10^8	0.25
Solid	22.7%	0.40 (60.3%) 6.66 (39.7%)	6.14	3.70×10^7	1.26×10^8	0.29

Table S5 Photophysical parameters of 4-APBA in THF, water and the solid state

	Φ_F (absolute)	τ (ns)	k_F (s^{-1})	k_{nr} (s^{-1})	k_F/k_{nr}
In THF	5.3%	3.67	1.46×10^7	2.58×10^8	0.056
In water	5.8%	0.31	1.89×10^8	3.08×10^9	0.061
Solid	5.6%	0.89	6.32×10^7	1.06×10^9	0.060

Table S6 Parameters obtained from ^{11}B MAS NMR lineshape simulation of solid 3-APBA sample

peak	δ_{iso} (ppm)	C_Q (MHZ)	η_Q	ratio
B[3]	27.8	3.1	0.5	83.3%
B[4]	1.9	–	–	16.7%

Table S7 Parameters obtained from ^{11}B MAS NMR lineshape simulation of solid 4-APBA sample

peak	δ_{iso} (ppm)	C_Q (MHZ)	η_Q	ratios
B[3]	27.7	2.9	0.52	45.5%
B[4]	18.5	2.5	0.3	28.3%
B[4]	1.7	–	–	26.2%

References:

1. Y. Ren, J. W. Y. Lam, Y. Dong, B. Z. Tang and K. S. Wong, *J. Phys. Chem. B*, 2005, **109**, 1135-1140.
2. Y. Qian, M. Cai, X. Zhou, Z. Gao, X. Wang, Y. Zhao, X. Yan, W. Wei, L. Xie and W. Huang, *J. Phys. Chem. C*, 2012, **116**, 12187-12195.
3. W. Jiang, C. Jiao, Y. Meng, L. Zhao, Q. Liu and T. Liu, *Chem. Sci.*, 2018, **9**, 617-622.
4. A. Hough, A. F. Routh, S. M. Clarke, P. V. Wiper, J. A. Amelse and L. Mafra, *J. Catal.*, 2016, **334**, 14-22.
5. S.-Y. Jiang, S.-X. Gan, X. Zhang, H. Li, Q.-Y. Qi, F.-Z. Cui, J. Lu and X. Zhao, *J. Am. Chem. Soc.*, 2019, **141**, 14981-14986.
6. R. A. Dragovic, C. Gardiner, A. S. Brooks, D. S. Tannetta, D. J. P. Ferguson, P. Hole, B. Carr, C. W. G. Redman, A. L. Harris, P. J. Dobson, P. Harrison and I. L. Sargent, *Nanomed-nanotechnol.*, 2011, **7**, 780-788.
7. Y. Tanaka and A. Ono, *Dalton T.*, 2008, 4965-4974.
8. E. Yuya, T. Yoshiyuki, G. Ryota, N. Satoshi, K. Yu, S. Naoki, N. Hiroko, S. Toshinobu and A. Jun-ichi, *Chem. Lett.*, 2010, **39**, 1188-1189.
9. K. A. Thorn, J. C. Pennington, K. R. Kennedy, L. G. Cox, C. A. Hayes and B. E. Porter, *Environ. Sci. Technol.*, 2008, **42**, 2542-2550.
10. R. Ma, B. Wang, P. Sun and L. Shi, *Chin. J. Chem.*, 2014, **32**, 97-102.
11. F. Wang, R. Zhang, Q. Wu, T. Chen, P. Sun and A.-C. Shi, *ACS Appl. Mater. Interfaces*, 2014, **6**, 21397-21407.
12. L. Zhu, S. H. Shabbir, M. Gray, V. M. Lynch, S. Sorey and E. V. Anslyn, *J. Am. Chem. Soc.*, 2006, **128**, 1222-1232.
13. S. F. Weng and Y. Z. Xu, in *Fourier Transform Infrared Spectrometry (Third Edition)*, eds. S. F. Weng and Y. Z. Xu, Chemical Industry Press, Beijing, 2016, pp. 250-252.